An Experimental and CFD Analysis of Pressure drop prediction in Dense-Phase Pneumatic Conveying of fine powders

A Dissertation submitted
in partial fulfillment of the requirements
for the of degree of

Master of Engineering

in

Thermal Engineering

by

Vikas

(Roll no.: 801583027)

Under the Supervision of

Dr. S. S. MALLICK (Associate Professor)

and

Mr. ATUL SHARMA (Lecturer)

DEPARTMENT OF MECHANICAL ENGINEERING

THAPAR UNIVERSITY, PATIALA

June, 2017

Certificate

I hereby declare that the thesis entitled "**An Experimental and CFD Analysis of Pressure drop prediction in Dense-Phase Pneumatic Conveying of fine powders**" is an authentic record of my own work carried out as per the requirements for the award of the degree of **Master of Engineering** in **Thermal Engineering** at **Thapar University, Patiala** under the supervision of **Dr S.S. Mallick (Associate Professor)** and **Mr. Atul Sharma (Lecturer)**, Mechanical Engineering Department Thapar University, Patiala during July, 2015 to July, 2017. No part of the matter embodied in this thesis report has been submitted to any other university or institute for the award of any degree.

Date: 14/7/17

Vikas

It is certified that the above statement made by the student is correct to the best of my /our knowledge and belief.

Dr S.S. Mallick
(Associate Professor)
Mechanical Engineering Department
Thapar University, Patiala-147004

Atul Sharma
(Lecturer)
Mechanical Engineering Department
Thapar University, Patiala-147004

i

Dedicated to

My Parents

Acknowledgements

Words often fall short to reveal one's deepest regards. I would be obliged to express my profound gratitude and respect to all the people who helped me throughout the duration of this work. Firstly I would like to express my sincere gratitude to Dr S. S. Mallick for his invaluable guidance and encouragement. I am also very thankful to Mr Atul Sharma, for his support and motivation in my research work.

I am also grateful to Prof. P.W. Wypych, University of Wollongong, Australia, for providing me the valuable information and relevant experimental data. All my colleagues in Thapar University are highly appreciated for their support for the research study as well as their social support, which has made my stay in Patiala enjoyable.

All India Council for Technical Education (AICTE) is also acknowledged for its financial support in the form of a scholarship to support the research work in the Thapar University.

Finally, I express my heartiest appreciation to my parents, my senior Amit Gupta Sir and my close friends Ritu Negi, Manu Dev Sharma and Nishant Kumar for their continuous encouragement and moral support.

Vikas

iii

Abstract

The present research work delves into CFD investigation of pressure drop for dense phase pneumatic conveying system of fine powders. In this study Computational fluid dynamics (CFD) principles have been used to determine the pressure drop across two straight pipes to explore the capabilities of simulation software for investigating into Pneumatic Conveying Characteristics (PCC) for fluidized dense phase pneumatic conveying of fly ash (mean particle diameter: 30μm; particle density: 2300kg/m^3; loose poured bulk density: 700kg/m^3). A commercial software code; Fluent® has been used for the investigation. Eulerian approach has been used for the simulation and the results show that the tested software can be used as an effective tool to determine the pressure drop in pneumatic conveying systems. Straight pipe pressure transducers installed at the two sections were used to provide the experimental pressure drop per unit length, which was used to form PCC for the experimental data. The results for pressure drop per unit length obtained from the simulations agreed reasonably well with experimental values of pressure drop, where average errors for both set of straight pipe simulations (69mm I.D. ×6m and 105mm I.D. ×6m) were found to be 21.55% and 15.66% respectively. PCC obtained from simulations were almost identical to the experimental PCC, which shows that though simulations were not performed on the original length of the pipe but still simulation results of pressure drop are in good agreement with the experimental results. The results of the effect of particle diameter, particle density and particle volume fraction on the pressure drop were also analysed. Also study of contours of flyash volume fraction for different particle diameter and particle density are reported in this study. The results of experimental PCCs of the research work carried on Thapar University pneumatic conveying test setup 50mm I.D. ×69m for grey cement and white cement as the conveying materials are also presented in this study.

Keywords: Pneumatic Conveying, Computational Fluid Dynamics, Pneumatic Conveying Characteristics etc.

Contents

Certificate ..... **Error! Bookmark not defined.**
Acknowledgements ..... **Error! Bookmark not defined.**
Abstract iii
Contents v
List of Figures vii
List of Tables ix
Nomenclature x
Chapter 1 1
Introduction 1
1.1 Introduction 1
1.2 Pneumatic Conveying and its components 1
1.3 Classification of pneumatic conveying 2
1.4 Applications of Pneumatic Conveying 4
1.5 Advantages of Pneumatic Conveying 5
1.6 Gas- Solid flow phenomenon in Pneumatic Conveying 5
1.7 Computational Fluid Dynamics (CFD) 6
1.8 Objectives of the research work 11
1.9 Outline of Thesis Work 11
Chapter 2 12
Literature Review 12
2.1 Introduction 12
2.2 Pneumatic Conveying Characteristics (PCC) 12
2.3 Design Parameters in Pneumatic conveying system 13
2.4 Computational Studies 14
2.5 Previous Research Work 15
2.6 Summary of Previous Research Works 18
Chapter 3 19
Experimental Investigation into pressure drop 19
3.1 Experimental Study on TU Test Setup 19
3.2 Properties of Materials 20
3.3 Calibration of Load cells and Pressure transducers 21
3.4 Calibration results for pressure transducers 21

3.5 Experimental Technique....24
3.6 Testing Methodology....24
3.7 Experimental Results of PCC for White cement and Grey Cement....25
Chapter 4....27
Methodology for Simulation study....27
4.1 CFD Simulation of straight pipe for Pressure drop prediction....27
4.2 Numerical Simulation....27
4.3 Pipe Geometry and Meshing....31
4.4 Grid Independence study....33
Chapter 5....35
Results & Discussions....35
5.1 Computational Investigation of pressure drop through CFD....35
5.2 Simulation results for 69mm I.D. × 6m and comparison with experimental data....35
5.3 Simulation results for 105mm I.D. × 6m and comparison with experimental data....37
5.4 Method to Plot PCC....39
5.5 Experimental PCC of flyash 69mm I.D. × 168m straight pipe....40
5.6 Simulation PCC of 69 mm I.D. ×6m straight pipe....41
5.7 Comparison of Experimental PCC of 69 mm I.D. ×168m and simulation PCC....42
5.8 Experimental PCC of 105mm I.D. ×168m straight pipe....43
5.9 Simulation PCC of 105mm I.D. × 6m straight pipe....44
5.10 Comparison of Experimental PCC of 105 mm I.D. ×168m and simulation PCC....45
5.11 Effect of particle diameter on the pressure drop....46
5.12 Effect of Particle density on pressure drop....47
5.13 Effect of Volume fraction on pressure drop....48
5.14 Results of contours of volume fraction of flyash at different particle diameter....49
5.15 Results of contours of volume fraction of flyash at different particle density....52
Chapter 6....55
Conclusion and Future Scope....55
6.1 Conclusion....55
6.2 Future Scope for Work....55
References....57
Web References....60
Appendix A....61

List of Figures

Figure 1.1	Schematic diagram of a typical dilute phase conveying system (The Basics of Pneumatic Conveying, 2017	3
Figure 1.2	Schematic diagram of a typical dense phase conveying system (The Basics of Pneumatic Conveying, 2017)	4
Figure 2.1	Typical Straight Pipe PCC FOR FLYASH 69mm I.D. ×168m (Mallick, 2010)	13
Figure 3.1	Schematic of Experimental test setup at Thapar University	19
Figure 3.2	Regression analysis of calibration on pressure transducers (P2-P8)	22
Figure 3.3	Experimental PCC for white cement (50mm I.D. ×69m) test rig	25
Figure 3.4	Experimental PCC for grey cement (50mm I.D. ×69m) test rig	26
Figure 4.1	Layout of the 69mm I.D. × 168m test rig for flyash	29
Figure 4.2	Layout of 105mm I.D. ×168m test rig for flyash	30
Figure 4.3	Convergence result of the scaled residuals	31
Figure 4.4	Geometry of 3D Straight Circular Pipe	32
Figure 4.5	3D Computational Grid	33
Figure 5.1	Comparison of Experimental (69mm I.D. ×168m) and simulated pressure gradient	37
Figure 5.2	Comparison of Experimental (105mm I.D. ×168m) and simulated pressure gradient	39
Figure 5.3	Experimental PCC of flyash (69mm I.D. ×168m)	41
Figure 5.4	Simulation PCC of flyash (69mm I.D. × 6m)	42
Figure 5.5	Comparison of Experimental PCC (69mm I.D. ×168m) vs Simulation PCC	43
Figure 5.6	Experimental PCC of flyash (105mm I.D. ×168m)	44
Figure 5.7	Simulation PCC of flyash (105mm I.D. × 6m)	45
Figure 5.8	Comparison of Experimental PCC (105mm I.D. ×168m) vs Simulation PCC	46
Figure 5.9	Effect of particle diameter on the pressure drop at different solid volume fraction	47
Figure 5.10	Effect of particle density on the pressure gradient at different particle diameter	48

Figure 5.11 Effect of particle volume fraction on pressure drop at different density 49
Figure 5.12 Contours of solid volume distribution at different particle diameter 51
Figure 5.13 Contours of solid volume distribution at different particle density 54

APPENDIX A

Figure A.1 Simulation Data points for PCC of 69 mm I.D. × 6m straight pipe 61
Figure A.2 Simulation data points for PCC of 105mm I.D. ×6m straight pipe 61
Figure A.3 Experimental data points for PCC of 69 mm I.D. × 168m straight pipe 62
Figure A.4 PCC of the experimental data points of 105 mm I.D. × 168m straight pipe 62

List of Tables

Table 3.1	Properties of materials and Particle Size Distribution	20
Table 3.2	Calibration results for pressure transducers	22
Table 4.1	Simulation factors	32
Table 5.1	Simulation results for (69mm I.D. × 6m) straight pipe	35
Table 5.2	Simulation results for (105mm I.D. × 6m) straight pipe	37

Nomenclature

V_f	Volume fraction of flyash
D	Internal diameter of pipe [m]
L	Length of pipe [m]
mf	Mass flow rate of air [kg/sec]
ms	Mass flow rate of solids [kg/sec]
m* = ms/mf	Solid loading Ratio
ΔP	Pressure drop through straight pipe [Pa]
ΔP_t	Interpolated pressure drop [Pa]
V	Superficial air velocity [m/sec]
ρ	Density of air [kg/m^3]
ρ_b	Bulk density of flyash [kg/m^3]
v_s	Volume flow rate of solid [m^3/sec]
v_a	Volume flow rate of air [m^3/sec]
λf	Friction factor for air
λs	Friction factor for solid

Chapter 1

Introduction

1.1 Introduction

Pneumatic conveying has appeared as one of the widely used technology for conveying bulk materials of different size and shapes. It is a method of conveying bulk particles with the help of carrier medium(gas) that are either suspended or non-suspended at single or multiple destinations through enclosed pipeline. In positive pressure based conveying, the gas stream which is usually the air is mainly generated from air compressor and air blower. The bulk materials generally transported are flyash, cement, pharma powders, food powders, sand, gypsum, silica etc. Having found its origin from Germany back in 1950s, it found its space in industries when R&D teams of Exxon, Union Carbide and Dow Chemicals of United States developed innovative ideas which made its use profoundly in various emerging industries (Sandy, 2016) be it food industries for conveying coffee beans, cereals etc. or power sector industries like power plant, cement, chemical and pharmaceutical industries. Although a number of numerical analysis have been carried out to model the flow phenomena in pneumatic conveying systems, only few attempts could be found where the CFD techniques have been used to predict the pressure drop of a pneumatic conveying system.

As a part of the present research, a CFD simulation was also included to investigate the pressure drop prediction capabilities of CFD software in the dense phase flow of a pneumatic conveying system.

1.2 Pneumatic Conveying and its components

Pneumatic conveying is a technique by which bulk materials (almost any type) are transported using conveying gas. The materials to be transported are conveyed through closed pipes conveying medium (provided by positive or negative pressure) and finally separated (with help of bag filters, cyclone separator) from gas and gathered at final destination (Ratnayke, 2005). The bulk materials exist in different forms including lumps, powder, granules and pellets. These materials require reliable material handling systems during their transportation. Coal and fly-ash in thermal power plants, sugar, chocolate powder and flour in food processing plants, zirconium and zirconium dioxide in nuclear power plants are well known bulk materials (Mallick, 2010).

Pneumatic conveying systems as explained by Ratnayke (2005) consist of four different zones where distinct operations are carried out. In each individual zone, some specialised equipment is required for successful operation of the plant. These components are discussed below:

- Conveying Gas Supply: Various types of compressors, fans, blower and vacuum pumps are used as prime mover for providing necessary energy for the conveying gas (Ratnayke, 2005)
- Feeding Mechanism: In order to feed the solid to the conveying line (a feeding mechanism such as Venturi feeder (low pressure <20kPa), rotary valve (low pressure<100kPa), screw feeder (medium pressure: 100 to 300kPa), Vacuum Nozzle (Negative pressure) & Blow tank (high pressure: 300 to 1000kPa) are used (Ratnayke, 2005)
- Conveying Line: This consists of all straight pipe lines horizontal and/ or vertical, bends and other auxiliary components such as valves.
- Separation Equipment: Separation equipment such as bag filters, and cyclone separator are used to separate solid from gas stream in which it has been transported (Ratnayke, 2005)

1.3 Classification of pneumatic conveying

On the basis of flow mechanism, pneumatic conveying is characterised into two main categories: dilute and dense phase (Mallick, 2010).

1.3.1 Dilute Phase Conveying

This mode of conveying uses large amount of air to move relatively small amount of particles (Wypych, 2006). Thus dilute phase is characterised by high velocity (more than 7.5 m/s) and low solid flow rates. Almost all kind of materials can be conveyed in this mode of conveying. Capital cost required in dilute phase is less, compared to other systems. It is also called suspended mode of conveying as solid particles almost remain suspended in high stream gas flow. Fig. 1.1 shows a schematic diagram of a typical dilute phase conveying system**.**

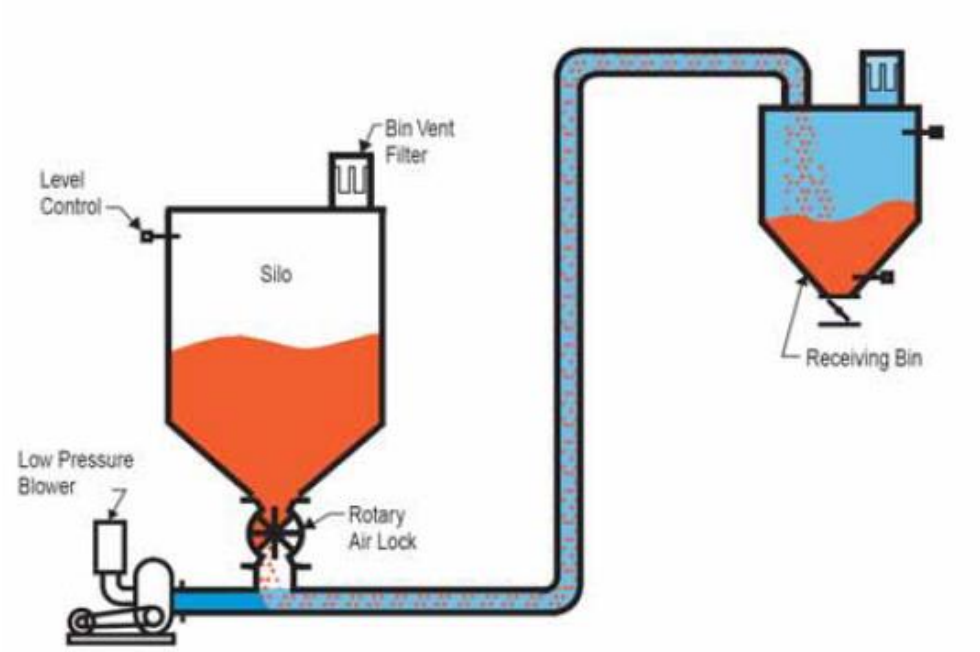

Figure 1.1: Schematic diagram of a typical dilute phase conveying system (Steele, 2005)

1.3.2 Dense Phase Conveying

This mode of conveying is characterised by low gas velocity to transport high solid flow rates, thus dense phase can push more solid particles at low air velocity (below saltation velocity). Saltation velocity is the velocity below which particles, no more remain in suspension. It has low power consumption and proven highly efficient system due to less air flow and more solid flow rates, thus reducing power consumption of compressor.

By reducing the gas velocity, bulk materials can be conveyed in stratification mode with varying concentration of solids. The material is forced through the pipeline as a plug, which occupies the cross section of pipe or travels as a moving bed for a pressure dependent distance (Silva et al., 2000). Even though there are different terms to define the different conveying patterns under reduced gas velocity, such as plug flow, slug flow, strand flow, moving beds, etc. in general, they all come under dense phase conveying. One such dense phase conveying system is given in Fig. 1.2.

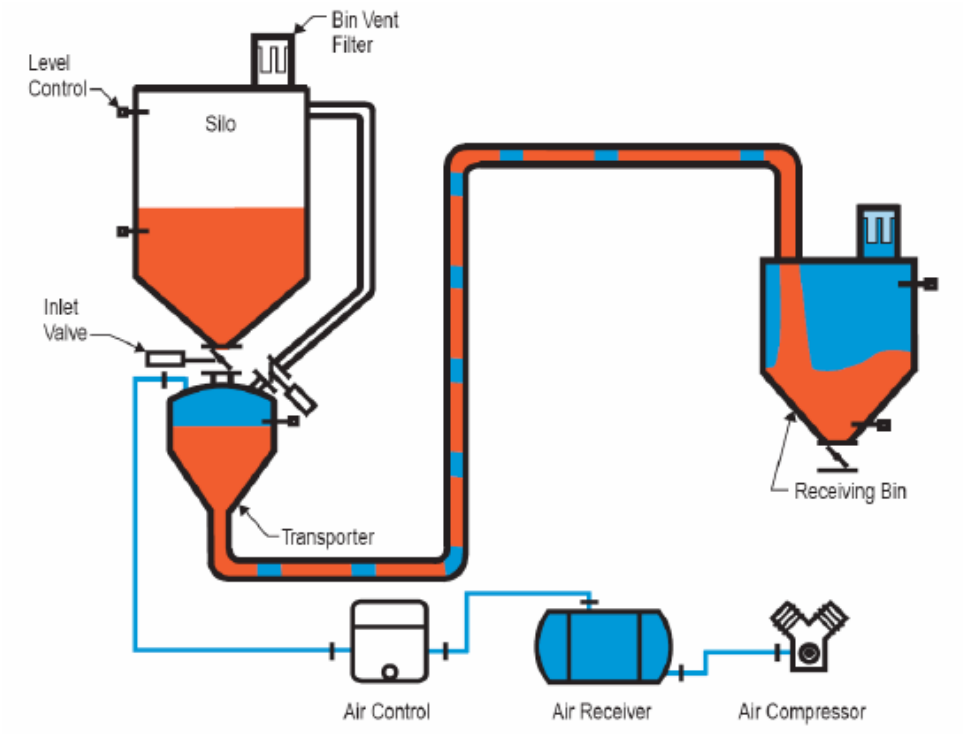

Figure 1.2: Schematic diagram of a typical dense phase conveying system (Steele, 2005)

1.4 Applications of Pneumatic Conveying

There are numerous applications of pneumatic conveying which find their profound use in various industries. Pneumatic conveying is used in various industries particularly used for Power Plant sector, Chemical Industries, Pharmaceutical Industries, Agriculture and Food Industries. Most of these industries use dilute phase conveying of variety of bulk and particulate materials. In terms of pressure conveying most of them use positive pressure or pressurised conveying through blow tank on the other hand pharmaceutical industries use vacuum conveying, as it requires clean transport of pharmaceutical powders. The size of particulate matter is rather not a constraint as it has been tested for almost very coarse materials of size 80mm like quartz to very fine materials such as talcum powders for size ranging between (30-60µm). Pneumatic Tubes/ Capsules are one of the recent applications of pneumatic transport which is used to transport solid objects over large distances (Liu, 2000). Nowadays it is used in United States as drive up banks for transporting cash and documents between cars and tellers (Andrew, 2004). It is also used in some hospitals to transport drugs and specimens from laboratories to nurse stations (Hamil and Sean, 2012). One of latest application of pneumatic tubes is for transport of passengers through Vactrain or Vacuum Tube Train (Giotta, 2011) &

Hyperloop (Musk, 2013). Researchers are working on this new technology for fast transport of passengers in evacuated tubes at speed more than 350 mph faster than BOEING passenger plane.

Well very soon with the success of Hyperloop One, the distance and time will not be a constraint to transport passengers via vacuum mode of conveying. The proposed structure of Hyperloop One has been constructed and will soon be in function in United Arab Emirates on Hyperloop routes (Reporters, 2017).

1.5 Advantages of Pneumatic Conveying

Pneumatic conveying framework has extensive variety of uses in various parts due to the following advantages (Klinzing et al., 2009)

i. Dust- free transportation of wide variety of bulk materials.
ii. Flexibility in routing – can be transported vertically and horizontally by the extension of a bend in the pipeline.
iii. Supply to and from different spots of the power plant.
iv. Low maintenance and labor costs.
v. Security – pipelines can be utilized to pass on valuable items.

Although pneumatic system has wide range of applications yet it has some limitations due to following (Klinzing et al., 2009)

i. High power utilization
ii. Deterioration and wear of pipeline due to abrasive nature of particles.
iii. Improper design can cause material degradation, underutilization and blockage in pipeline.
iv. Limited distance for conveying of bulk material.

1.6 Gas- Solid flow phenomenon in Pneumatic Conveying

Gas-Solid flow applications in pipe are seen in many industries such as pneumatic conveying, fluidized beds, pulverised bed combustion etc. Parameters such as mass flow rate of air, volumetric concentration and particle and air velocity should be calculated and regulated precisely for efficient energy utilization. Henceforth a great interest is developed in the study of gas solid investigation over couple of years. The prediction of pressure drop is significant for the analysis of pneumatic system. In case of horizontal pipes gravitational effects are predominant which causes more particles at the bottom of pipe resulting in particle wall interactions. Hence flow is quite complex in horizontal pipes than vertical pipes. Owing to great

requirement of gas solid flow for achieving proficiency of good technical design and less energy consumption in pneumatic conveying, there has been lot of research work over the last few decades.

As a consequence, many experimental studies are needed to understand the gas-solid flow phenomenon in pneumatic conveying system. With the advent of high speed computer applications researchers, scientists and engineers find their ease in visualising the complex flow phenomenon and predicting pressure drop in pneumatic conveying system.

1.7 Computational Fluid Dynamics (CFD)

Over the few years, CFD has developed as an important simulation tool for the investigation of gas-solid flow systems comprising fluid flow problems. Computers serve as the communicating mode to define interactive forces between solid and gas which are initialised by some boundary conditions. Higher is the processor speed of the computer better simulation results can be attained. The accuracy of simulation results depends on the discretization scheme, physical model and selection of correct simulation parameters and boundary conditions. CFD has thus found its way into thermal, heat transfer, structural and advance fluid mechanics study. Some of the widely used commercial CFD packages are: FLUENT, ANSYSCFX, ANSYS ICEM, STARCD, STARCCM, COMSOL, Open FOAM, KIVA etc. The physical aspect of the inbuilt CFD codes is determined by three principles: Conservation of Mass, Momentum and Energy. These fundamental principles of fluid mechanics are represented in terms of basic mathematical expressions, which are either in form of integral equations or Partial Differential Equations (PDEs). CFD is thus an art of replacing integral or partial derivatives in these equations with discretized algebraic forms which in turn are used to find fluid flow values in terms of numbers at any discrete point in space and time.

1.7.1 Advantages of CFD

CFD provides a prediction into complex flow patterns which are cumbersome and impossible to study using experimental techniques. Some of the advantages of CFD over experimental techniques are as follows:

1) It provides faster and more economical solution than physical modeling.
2) CFD can visualise complex flow conditions that cannot be observed in experimental tests.

3) CFD can help the design engineer in improving product designs by determining the flow behavior before constructing a physical prototype, which saves time, labor, and money.

1.7.2 Applications of CFD

There are numerous usages of CFD. Some of them are few of applications associated with CFD:

1) The architects can design comfortable and risk free environment through structural analysis.
2) The automobile designers can improve vehicle aerodynamic features
3) The surgeons can cure blood vessel ailments (computational haemodynamic)
4) The safety experts can lower risk from radiation.
5) The defence organizations can develop weapons and can minimise the risks of attacks from enemies.

1.7.3 Basic modules of CFD

There are various basic modules of CFD which need to be understand before carrying out the simulation study, some of them are described below:

1.7.3.1 Mathematical Model

A perfect mathematical model which consists of suitable PDEs and boundary conditions is the starting point of any numerical modelling**.**

1.7.3.2 Discretization Technique

After using appropriate mathematical model, a suitable discretization scheme should be selected. Discretization is a process of approximating the PDEs or integral equations into a set of algebraic equations. There are different discretization methods: Finite Difference Method, Finite Element Method and Finite Volume Method. Each method provides similar results if the meshing or grid is fine.

1.7.3.3 Numerical Grid

The distinct locations at which variables to be calculated are defined by numerical grid, which is nothing but the discrete representation of the geometric domain, in which the problem is to be solved. It basically divides the final solution domains into smaller sub domains. There are

basically three numerical grids: Structured grids, Unstructured Grids and Block Structured Grids. Some of the grid generation softwares are: ANSYS Workbench, ICEM CFD, GRIDGEN, TGRID, GMSH, GAMBIT etc.

In structured grids the family of numerical grid lines has the basic property that members of the single family do not cross each other and can only cross other family grid lines once. This allows lines for a given set to be numbered consecutively. The position of the grid point in any domain is either defined by two nodal points for a 2D form or by three indices in 3D form. This is the simplest meshing scheme as it is logically similar to Cartesian grid. Each nodal point has 3 nearest neighbours in 2D and six nearest neighbours for 3D. Each neighbouring nodal point differs by ± 1 from corresponding next neighbour nodal point. Structured grids have some disadvantages than other grids. Some of them are:

1) They can only be used for simple geometrical domain
2) It is difficult to control the distribution of grid points. In order to control the accuracy it causes concentration of points at a particular region. This results into unnecessary spacing at other points in same geometric domain causing wastage of resources
3) The long thin cells may adversely affect the convergence
4) The structured grids could be of H, C & O types. These names are derived from the shapes of grid lines.

Unstructured grids are relatively the most flexible types of numerical grids as they are used for complex geometries and can easily fit into an arbitrary solution domain. Such grids are adaptable for any discretization scheme but the best results are obtained if used with finite volume and finite element approaches. The numerical codes for unstructured grids are more flexible.

Block Structured grids consist two or more subdivision of the solution domain. On the coarse level, the blocks are relatively larger section of domain. The geometric structures in block structured grids are mostly irregular. The block centred grids having overlapping blocks are mainly called composite or chimera grids.

1.7.3.4 Finite Approximations

Following the choice of discretization scheme, it is required to select the approximation to be used in the discretization. In Finite Volume method, the approximations for mainly surface and volume integral are solved. In Finite Element method, the shape and weighing function are

chosen. In finite difference method, the numerical approximations for finite derivatives at grid points must be selected.

1.7.3.5 Solution Methodology

Discretization leads to formation of large system of nonlinear algebraic equations. The method of solution depends on the choice of grid, boundary conditions and mathematical models. The accurate choice of solver depends on the type of the grid and the number of nodes involved in each algebraic equation.

1.7.3.6 Convergence Criteria

The numerical modelling technique requires ways to measure the accuracy of the simulation result. Hence, convergence criteria for each iterative method must be suitably set, which depends entirely on type of models selected as per the problem to be solved. The convergence residuals for continuity, energy and turbulence and epsilon need to be defined depending on type of model selected.

1.7.4 Stages in CFD Simulation

Although every sets of simulation case varies in accordance with the end results, it is also true that the number of steps to be followed remains almost similar. The main stages in CFD simulation as described by Patel, 2017 are given below**:**

1.7.4.1 Define the Modelling Objective

Before executing the analysis, it is important to understand the objectives which are to be fulfilled through CFD. It is necessary to note down the objectives, modelling options required, physical models, boundary conditions and accuracy of result required.

1.7.4.2 Defining the Geometry

After gathering needful information, next stage is defining appropriate geometry based on assumption made. Developing the geometry can be done either by in built Geometry builder in CFD software package, or by some other design software which could be later imported for analysis.

1.7.4.3 Defining and Creating Mesh

Meshing is one of the prime stage of CFD simulation and it should be accurate enough to consider the complexity of geometry and flow. Mesh should be refined on the regions of high gradients for accuracy of results.

1.7.4.4 Setting the solver

Next stage to meshing, is to decide type of solver needed (pressure based, density based, steady, unsteady) to address the specific problem. Subsequently it is required to select the appropriate physical model (Turbulence, Multiphase etc.) based on the problem defined. After selecting suitable model and solver material properties, operating conditions and boundary conditions should be defined. Convergence criteria also needs to be defined followed by flow field initialisation.

1.7.4.5 Monitoring the Solution

It is necessary to monitor the solution during computing, while the iterations are executed. The solution is converged when no change in variables is found after several iterations. Monitoring the solution helps to keep track of accuracy of physical model, meshing and problem setup.

1.7.4.6 Evaluating the Solution through Results

Evaluating the solution and extracting the results help in analysing the problem setup. With visualisation and numerical reporting tools, one can easily identify the flow pattern, separation phenomenon, pressure drop, heat transfer and flux quantities.

1.7.4.7 Reassessing the Model

Based on the results obtained, next step is the analysing the appropriateness of the physical model and solver selected. Also the accuracy of the boundary conditions and meshing can be assessed through results. If the results obtained are not as per the expectations, reassessing should be carried out by varying the solver and physical models, refining the mesh and opting new boundary conditions.

1.8 Objectives of the research work

The main objectives of research work in this study are presented below:

1) To perform CFD simulations for finding pressure drop through straight pipe using experimental data from test setup of University of Wollongong, Australia and draw PCC of the simulation results of pressure drop and also comparing the results with experimental PCC.
2) To utilise the capability of CFD software for finding the effect of particle diameter, particle volume fraction, air velocity on the pressure drop through straight pipe.
3) To perform experiments on TU pneumatic conveying test setup for different conveying materials (grey cement, white cement) and draw PCC of the experimental data.

1.9 Outline of Thesis Work

Chapter 1 includes introduction on Pneumatic Conveying and its classifications and applications and a detailed explanation of basics of Computational Fluid Dynamics, Objectives of present research work and Thesis Outline.

Chapter 2 covers Literature review of previous research work.

Chapter 3 provides details about Thapar University experimental test setup and results of PCC of the experimental pressure drop per unit length of total pipeline pressure drop for white cement and grey cement

Chapter 4 details the numerical solution steps of the pressure drop prediction. The proper selection of solver and models, material selection in CFD and its properties, boundary condition and convergence criteria used for simulation are discussed under numerical simulation. It also gives details about pipe geometry and mesh and grid independence study.

Chapter 5 deals with the simulation results of pressure drop and the percentage errors in experimental & simulated pressure drop. The experimental and simulated PCC and their comparison are also presented. Also the effects of parameters such as particle diameter, particle density and volume fraction on pressure drop and solid volume distribution is presented.

Chapter 6 includes overall conclusion and future scope for the study.

.

Chapter 2

Literature Review

2.1 Introduction

The purpose of this chapter is to present a review of the various studies conducted over the years (by different researchers) on the subject of computational study through CFD for prediction of pressure drop in dense phase pneumatic conveying. Initial studies done during the thesis are related to concepts on pneumatic conveying characteristics, design parameters and computational studies. Further research work is primarily focused on the review of papers on the applications of CFD for pressure drop calculation and simulation study of the effects of various parameters such as particle diameter, particle density and particle volume fraction on the pressure drop. The brief details about these studies are presented below:

2.2 Pneumatic Conveying Characteristics (PCC)

Pneumatic conveying characteristics (PCC) provides an essential requirement for the reliable design of pneumatic transportation systems (Wypych and Arnold, 1985). Steady state pipeline conveying characteristics can provide valuable information, such as the expected mode of flow condition (dilute/dense) for a particular combination of ms and mf, minimum conveying air velocity (either for dense- or dilute-phase) and the optimal operating conditions for a given product (Mallick, 2010). PCC curves are representation of a given product that is conveyed pneumatically i.e. variation of pressure drop per unit length for a range of air flow rate at a given tonnage.

Figure 2.1 shows PCC for flyash conveyed through 69mm I.D. ×168m straight pipe (Mallick, 2010). It is a plot for pressure gradient (ΔP/L) on Y axis and mass flow rate of air (m_a) on X axis at different tonnage of solid.

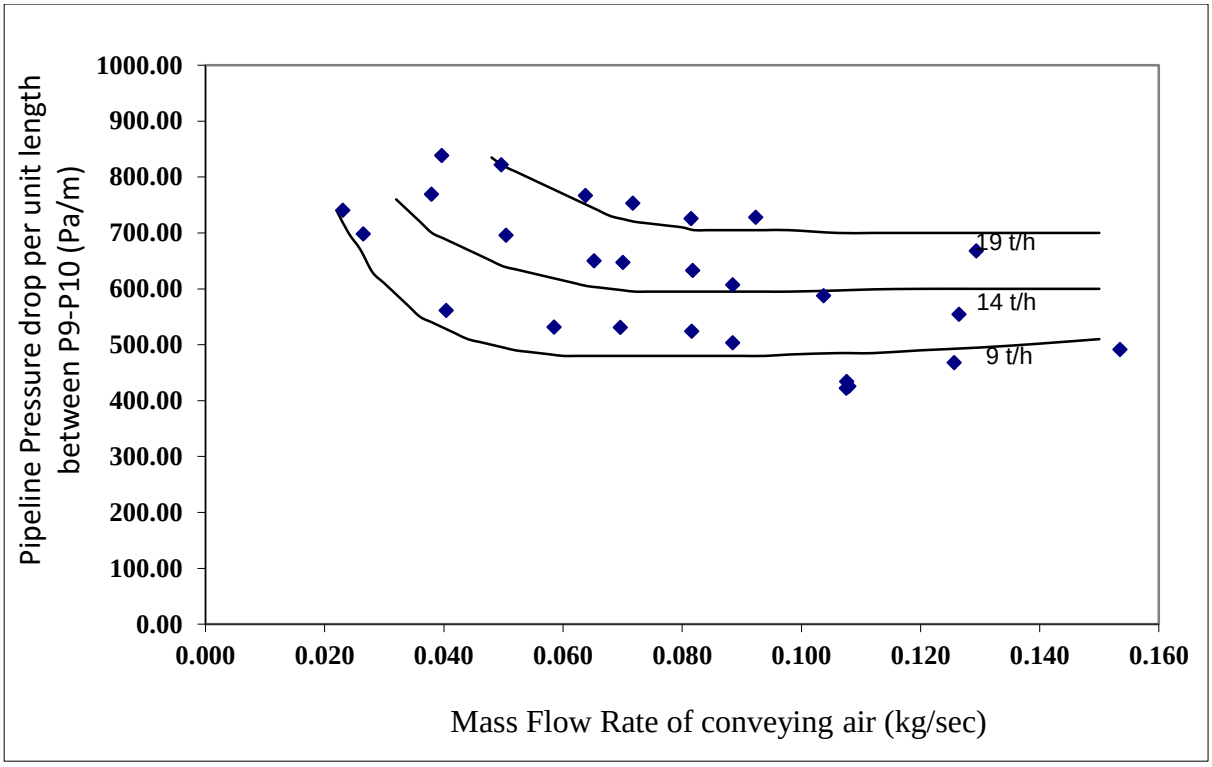

Figure 2.1: Typical Straight Pipe PCC FOR FLYASH 69mm I.D.× 168m (Mallick, 2010)

2.3 Design Parameters in Pneumatic conveying system

Basically two important parameters, pressure drop across pipeline and Pressure Minimum Curve are required to be studied prior to the design of reliable pneumatic conveying setup (Ratnayke, 2005). These parameters are studied mathematically through various models and correlations of pressure drop. A lot of research work has been done on numerical modelling of pressure drop. But research work in this thesis is focussed mainly on utilising the simulation techniques of commercial CFD code to predict the pressure drop across straight pipe and then generating PCC of pressure drop obtained through simulation. Moreover the simulation study on the effects of various parameters such as particle diameter, volume fraction and particle density on the pressure drop is also conducted.

2.3.1 Pressure drop through straight pipe

One of the earlier researchers to propose a mathematical expression for finding pressure drop for solid-gas flow in a straight horizontal pipe was Barth (1958). He considered that total losses due to the solids- gas mixture can be represented as the sum of individual losses due to the solids and gas only, as given by Eq. (2.1).

$$\Delta P = \frac{(\lambda_f + m^* \lambda_s) L \rho V^2}{2D} \quad (2.1)$$

However, this equation has been used subsequently by various researchers (Stegmaier, 1978; Rizk, 1976, 1982; Pan, 1992; Pan and Wypych, 1998; Wypych, 1989; Jones and Williams, 2003; Williams and Jones, 2004) to predict the pressure loss for dense-phase flow of fine powders, such as fly ash. Undoubtedly, Barth's representation has remained the most popular and fundamental equation for accounting solids friction in pneumatic conveying systems (dilute- and fluidised dense-phase).

2.4 Computational Studies

Over the last few years, computer skilfulness has well received as a useful technique for studying multiphase processes. With the growth of high speed computers, scientists and researchers have adequately been using these computer codes for understanding and visualising the complex flow phenomenon of dense phase pneumatic conveying systems which are otherwise difficult to understand with the traditional techniques. But, unfortunately, very few research papers could be noticed in open literature, which explores the potential of computer codes in commercial CFD software for prediction of pressure drop in dense phase pneumatic conveying system.

CFD includes numerical solution of sets of governing differential equations, and other equations as required. CFD has so far proven to be useful for investigation of single phase flow problems. It is thus possible to make predictions for single phase flow which are more accurate than the experimental measurements of the same physical setup of the given geometry. There are two numerical approaches to solve gas-solid flow problems for particulate matter: Eulerian-Lagrangian approach and Eulerian-Eulerian approach. While Lagrangian approach is more suitable for dilute flow problems and is not used for large number of particles, Eulerian approach is used for dense flow problems. Few investigations which endeavoured to predict the gas-solid flow behaviour using Eulerian -Eulerian approach came out with remarkable results (Scott (1978), Manger (1996), Mathiesen (1997), Wang (2001)).

In current years, development could be achieved, particularly in the CFD applications of dense phase gas-solid flow system, when some research work (Jenkins & Savage (1983), Lun et al. (1984), Johanson & Jackson (1987), Ding and Gidaspow (1990)) developed relations for inter particle interactions. Although, a lot of research papers of CFD in dilute phase pneumatic conveying system (Yasuna et al. (1995), Mason et al. (1998), Li and Tomita (2000),

Sommerfeld et al. (2001)) and fluidised bed system (Mathiesen (1997), Benyahia et al. (2000), Mathiesen and Solberg (2004), Ye et al. (2004)) can be seen in open literature, though the application in dense phase pneumatic conveying is comparatively less. Although there are some commercial CFD codes which claim better implementation in dense phase conveying applications but their usability in real situations is limited. On the contrary, only a few cases (Levy et al. (1997), Giddings et al. (2004), Ye et al. (2004)) could be found where some attempts were made to use CFD codes to predict pressure drops across the gas- solid flow systems.

2.5 Previous Research Work

This research work, is related to simulating flow phenomenon in pneumatic conveying through CFD and also experimental tests, both having similar objectives of making PCC of the experimental and simulation results. Research works of some previous researchers that helped in giving the right direction for this research study are presented below:

Tsuji et al. (1991) implemented CFD simulation of multiphase flow on horizontal straight pipe using Lagrangian approach taking particles of different shapes, however the results were found accurate only for particles with spherical shape. In actual two phase simulation particle shape and size are much in variety and hence for comparison of results between experiments and simulation shape of particles should be taken into consideration.

Levy and Mason (2000) studied dense phase multiphase flow through horizontal pipe by using two layer model (dispersed and dense flow). Later, Mason and Levy (2001) used the same model to study dense phase conveying of small size particles and affirmed better predicted results of pressure drop with experimentally defined pressure profiles for dense phase pneumatic conveying of horizontal pipes. Many investigators e.g. Sommerfeld and Kussin (2004), Lain and Sommerfeld (2011) and Lain and Sommerfeld (2012) studied the numerical multiphase flow involving solid particles with gas in straight pipe with different configurations

Zhu et al. (2004) performed numerical study on the effects of conveying of granular particles at different inclinations of the pipe through CFD simulation. It was reported in the results that inclination angle have significant influence on the solid volume distribution over the cross section of the pipe for the large granular particles. Solid distribution in the form of wave was

observed with axial depressions when a little amount of sinusoidal fluctuation in the gas velocity was introduced at entry to the pipe.

Heinl and Bohnet (2005) performed CFD simulations on a horizontal pipe of length 3m and 50mm inner diameter taking into account of wall and particle interactions. The significant influence of distinct wall conditions on the pressure drop and particle wall interactions was studied by using Lagrangian approach for the dispersed particle phase and turbulence 2 equation (k-ε) model for the gas phase. User defined functions were also used to implement models not provided by the Fluent. The results of simulation are validated with measured experimental data.

Ratnayke et al. (2005) performed CFD simulations on pipe bend for pressure drop prediction using two different fine powders (cement and ilmenite) and with different pipe configurations. The Eulerian modelling shows that predicted values of pressure drop agrees well with the experimental pressure drop values having maximum error margin of ±15% for dense phase pneumatic conveying. The contour results of solid volume fraction shows high solid volume concentration at the long radius wall of the bend and in the vicinity of outlet, similar high solid volume concentration could be seen at the bottom area of the conveying pipe. The cross sectional contour plots shows that high particle concentration slides gradually from the long radius side wall to the lower half of the pipe along the pipeline due to the centrifugal forces of solid particles, which diminishes slowly and is countered by gravitational forces that causes settling of solid particles at the bottom of the cross section of the pipe.

Mcglinchey et al. (2007) used Eulerian modelling to predict pressure drop in the bend by carrying out simulation using Ansys Fluent software. Author performed simulation work on horizontal and vertically 90° bends of 1m bend radius. Author used Eulerian and mixture models and compared simulation results with experimental data. From experimental results author showed that for higher solid loading ratio, the Eulerian modelling with unsteady approach provides good results within 50% of measured values, but this approach was not good for vertical bends and shows under prediction from the measured values while for lower solid loading ratios the mixture multiphase and steady state approach were more suitable for vertical bends and shows good results within 50% of the measure value. For horizontal bend mixture model underestimate by a factor of around three.

Ma et al. (2010) conducted CFD simulations to study multiphase flow phenomenon in dense phase pneumatic conveying systems for predicting pressure drop. The calculated results of pressure gradient are in accordance with experimental pressure drop. The results also shows that pressure gradient increases with the increase in particle diameter and particle density. Roughness height and bend curvature ratio has a major effect on pressure gradient, as the pressure gradient rises with roughness height and decreases with increase in bend curvature ratio.

Kartushinsky et al. (2011) investigated multiphase flow phenomenon in horizontal pipe through simulation techniques and observed that presence of solid particles in the entrained flow causes change in the flow phenomenon. The simulation result shows that gas flow becomes mainly asymmetric because of phenomenon of sedimentation of particles along the periphery of the pipe. Also presence of the solid particles has a significant effect on all the flow profiles including the turbulence intensity distribution. The 3D two-phase flow modeling is of high relevance for some natural phenomena, where the effects of gravity result in the flow asymmetry.

Liu et al. (2011) conducted CFD simulation of dense phase conveying of flyash for a long distance pipe. The key results of CFD simulation shows that the dynamic pressure decreases on the upper end of pipe while opposite effect was observed at the bottom end due to high particle concentration. Gas and particle velocities at the upper end of pipe is large compared to the bottom end.

Behera et al. (2013) conducted simulation through CFD for predicting pressure drop in dense phase pneumatic conveying of fine particles. They simulated a horizontal pipe of length 2m to study the void fraction distribution of particles at the outlet cross section of the pipe. The predicted pressure drop of some values of experimental data points for 173m long experimental setup showed good agreements with experimental pressure drop as the predicted pressure drop values had an average error in pressure drop of 11.02% with standard deviation of 10.38%. The solid void fraction increases from bottom to top layers across the cross-section of the pipeline but the solids volume fraction for different layers was quite lower at 100m location as compared to that at 29 m location.

Mcglinchey et al. (2012) performed CFD simulation in stepped pipe to investigate dense phase flow using Eulerian approach. Results indicate a reasonable representation of pressure drop and solids concentrations. The results indicated that an abrupt expansion may result in a plug which has passed through the step having increased aeration which will be beneficial for fine powders. Whereas for the gradual expansion case the plug was seen to collapse and elongate based on patterns of solids volume fraction with a potential for plug de-aeration and eventual pipeline blockage.

Kumar et al. (2014) investigated pressure drop prediction capabilities of CFD simulation across bend using cement as the conveying material for different conveying conditions. The key results obtained shows that pressure gradient across bend increases with increase in solid concentration and flow velocity, which is mainly due to increased particle interactions at higher velocities and solid concentration. The contour results shows large solid concentration is present at the outer wall of the bend radius. The main analysis of the results can be seen in the form of applicability of Eulerian multiphase model and transient analysis at high solid loading ratio whereas at low solid loading ratio, usually Mixture model and steady state analysis were used for the horizontal bend.

`

2.6 Summary of Previous Research Works

- Most of the research papers on pneumatic conveying of gas-solid flow used relatively large particles instead particles of smaller size.
- CFD simulation of multiphase flow in straight pipe is less reported in literature.
- Although lot of experimental PCC for pipeline pressure drop are available, less work has been reported on CFD simulation to predict pressure drop and plot simulation PCC.
- Most of the simulation study was done for flow visualisation in pneumatic conveying but few researchers presented calculation of pressure drop for large range of data instead used only few data points for calculation of pressure drop.

Chapter 3

Experimental Investigation into pressure drop

3.1 Experimental Study on TU Test Setup

The research work in this thesis apart from simulation study of pressure drop, also takes into account of the experimental investigation into the total pipeline pressure drop of fine powders and the results of experimental pressure drop are used to draw PCC for total pipeline pressure drop. For the experimental studies, the Pneumatic conveying test facility at Laboratory of Bulk Solid and Handling, Department of Mechanical Engineering is provided. The test rig consists of 50mm I.D. ×69m loop having six bends as shown in Fig. 3.1.

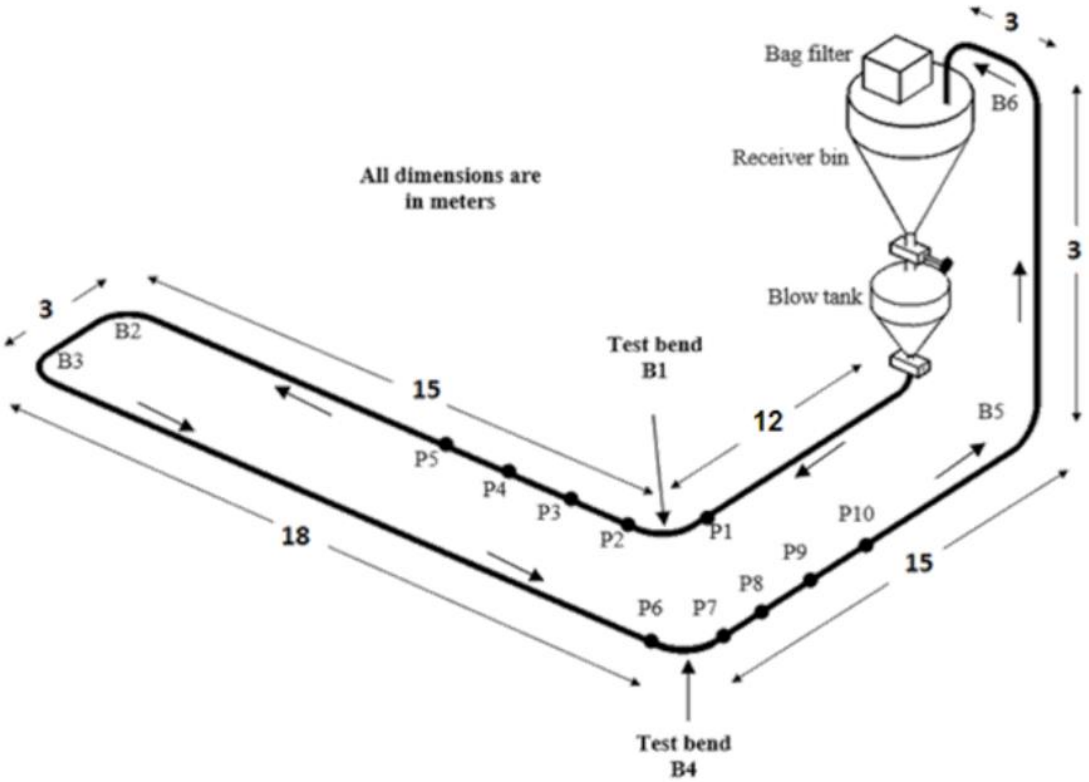

Figure 3.1: Schematic of Experimental test setup at Thapar University

A schematic diagram of the test setup is shown in Fig. 3.1. Major components of the test setup are as follows:

- Rotary screw compressor (Model: KES 18-7.5) with maximum pressure limit of 750kPa and free air delivery of 3.37 m^3/min.

- 0.5 m^3 receiving hopper installed with bag filter at its top to separate material from air.
- 0.2 m^3 capacity blow tank with maximum working pressure of 400kPa.
- 70m long pipeline with 50mm internal diameter.
- Data Acquisition System.
- PLC and pneumatic control panel

Five pressure transducers (P1 TO P5) as shown in above figure, were used to take the pressure readings at both static and steady conditions. Receiver bin was mounted over blow tank with a pulse jet bag filter. The compressed air was dehumidified with a refrigerated type of air dryer. A storage tank for compressed air having capacity of $2m^3$ was used to overcome erratic supply of compressed air. Other useful instruments such as pressure reducing valve, blow valve, flow meter, and pressure gauge and load cells were used to quantify the solid flow rate. Also an AD (Analog to Digital) data acquisition system is used to convert current signal of pressure into corresponding digital values of pressure. In this study, two materials were used namely grey cement and white cement whose physical properties are given in Table 3.1

3.2 Properties of Materials

Table 3.1 shows the properties of the materials used in the study at different particle diameters. The two materials used in this study are grey cement and white cement. Mean particle diameter for white cement is 19µm while for grey cement is 18µm. Particle and bulk densities of grey cement are almost closer to white cement.

Table 3.1: Properties of Materials and Particle Size Distribution

Product	ρ_b **(kg/m^3)**	ρ_p **(kg/m^3)**	d_{50} **(µm)**	d_{10} **(µm)**	d_{90} **(µm)**
White Cement	1028	2720	19	3	50
	1028	2720	19	3	50
	1028	2720	19	3	50
	1028	2720	19	3	50
	1028	2720	19	3	50
Grey Cement	1020	2680	18	3	53
	1020	2680	18	3	53
	1020	2680	18	3	53
	1020	2680	18	3	53
	1020	2680	18	3	53

3.3 Calibration of Load cells and Pressure transducers

Load cells and pressure transducers were used to measure mass flow rate and static pressure in a cycle. Load cells generate voltage signal and pressure transducers current signals which are then converted to corresponding load and pressure reading with the help of a calibration factor. Calibration of load cells and pressure transducers are done with the help of a standard procedure described by Pan (1992). For the calibration of pressure transducers following steps are followed:

1) Connect all pressure transducers via cables to the data acquisition system.
2) With all the material in the receiver bin, purging (pumping air only through the pipeline) is done keeping all the material inlet valves, ball valve, vent valve closed and only keeping discharge valve open.
3) After closing the blind flange which is upstream of the material feed point, increase the pressure in the line upto 200kPa.
4) Check for the leakage in the pipeline, if there is leakage at some point then open the vent valve to avoid the possible leakage.
5) Next, close the vent valve and increase the pressure and note down current readings from pressure transducers.
6) Open the inlet valve after first five readings of pressure.
7) Next, plot graph of pressure transducers corresponding to current values.
8) Draw linear trend lines and note down the displayed equations & the values of calibration factor.

3.4 Calibration results for pressure transducers

Table 3.2 shows calibration results for pressure transducers in the form of current which will be used to provide calibrated values of pressure after regression analysis. The values of calibration factors displayed in the equation given in the regression curves are replaced into NI data logger equations to give calibrated values of pressure.

Specifications of Pressure Transducers: Make: Endress+Hauser^{TM}, Model: Cerabar TPMC131, range of pressure: 4bar-2bar, Range of current: 4-20mA

Table 3.2: Calibration results for pressure transducers

P2	P3	P4	P5	P7	P8	Pressure (bar)
0.0093669	0.0148163	0.014817	0.014806	0.0148448	0.0147849	1.5
0.00892787	0.0139446	0.0139454	0.0139357	0.0139718	0.0139123	1.4
0.00853378	0.0131582	0.0131611	0.0131507	0.0131848	0.0131314	1.3
0.00816758	0.0124308	0.0124314	0.0124185	0.0124525	0.0123995	1.2
0.00780324	0.0116968	0.0116992	0.0116891	0.0117199	0.0116674	1.1
0.00740587	0.0109006	0.0109	0.0108922	0.0109224	0.0108705	1

The linear trend lines of pressure transducers (P2-P8) with the calibration factors are shown in Fig. 3.2.

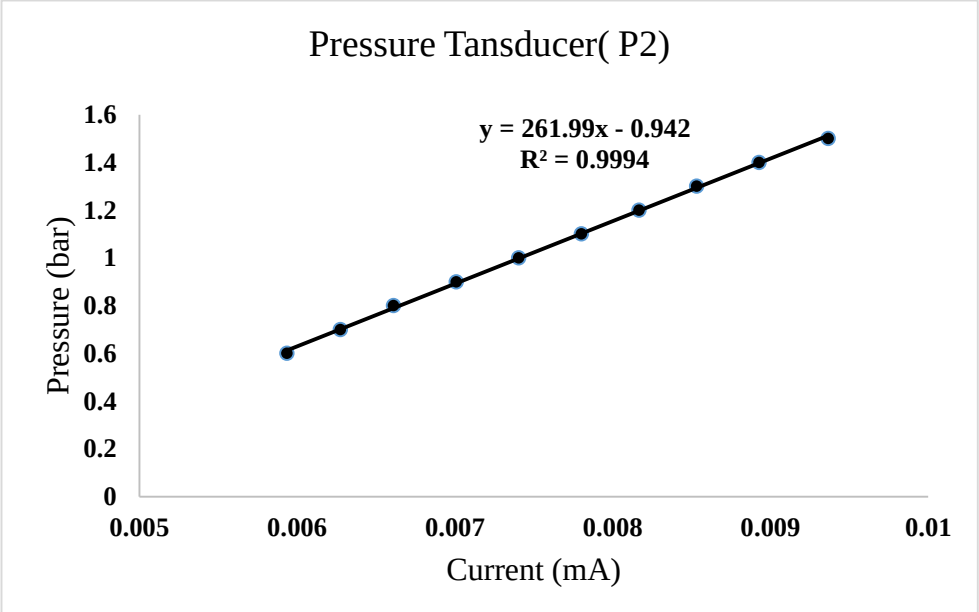

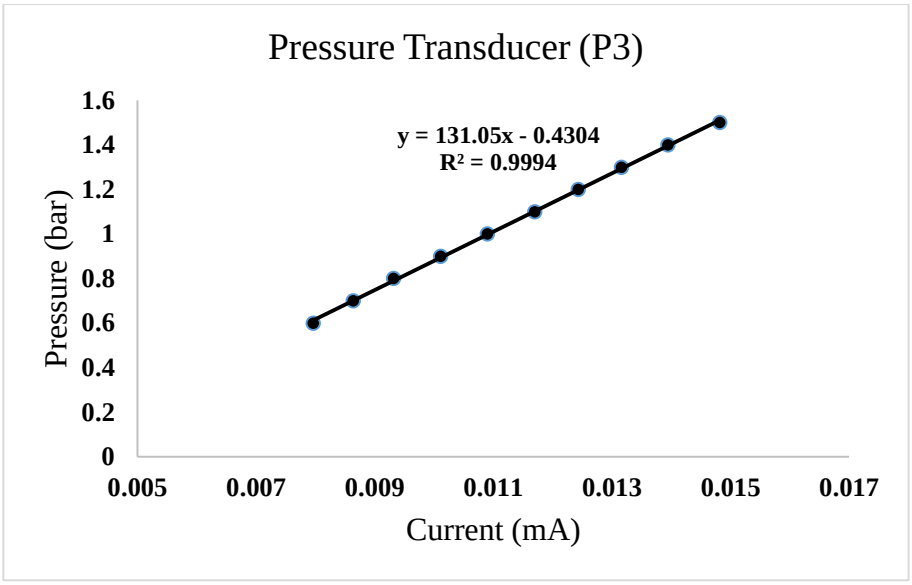
Pressure Transducer (P3)
y = 131.05x - 0.4304
R² = 0.9994
Pressure (bar)
1.6
1.4
1.2
1
0.8
0.6
0.4
0.2
0
0.005
0.007
0.009
0.011
0.013
0.015
0.017
Current (mA)

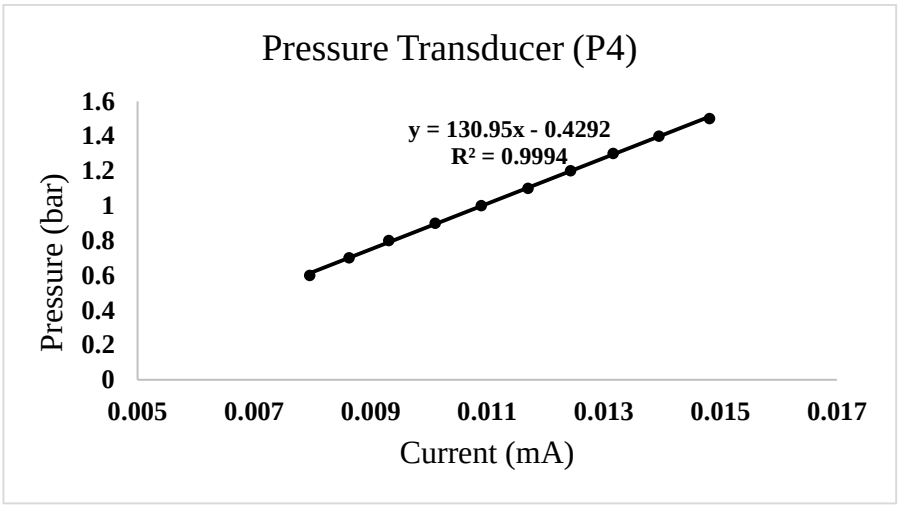
Pressure Transducer (P4)
y = 130.95x - 0.4292
R² = 0.9994
Pressure (bar)
1.6
1.4
1.2
1
0.8
0.6
0.4
0.2
0
0.005
0.007
0.009
0.011
0.013
0.015
0.017
Current (mA)

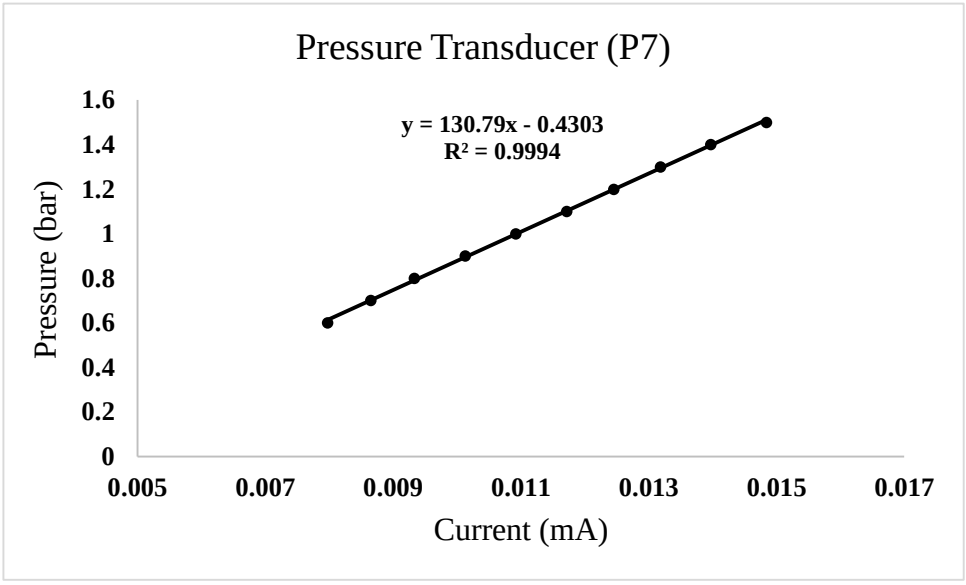
Pressure Transducer (P7)
y = 130.79x - 0.4303
R² = 0.9994
Pressure (bar)
1.6
1.4
1.2
1
0.8
0.6
0.4
0.2
0
0.005
0.007
0.009
0.011
0.013
0.015
0.017
Current (mA)

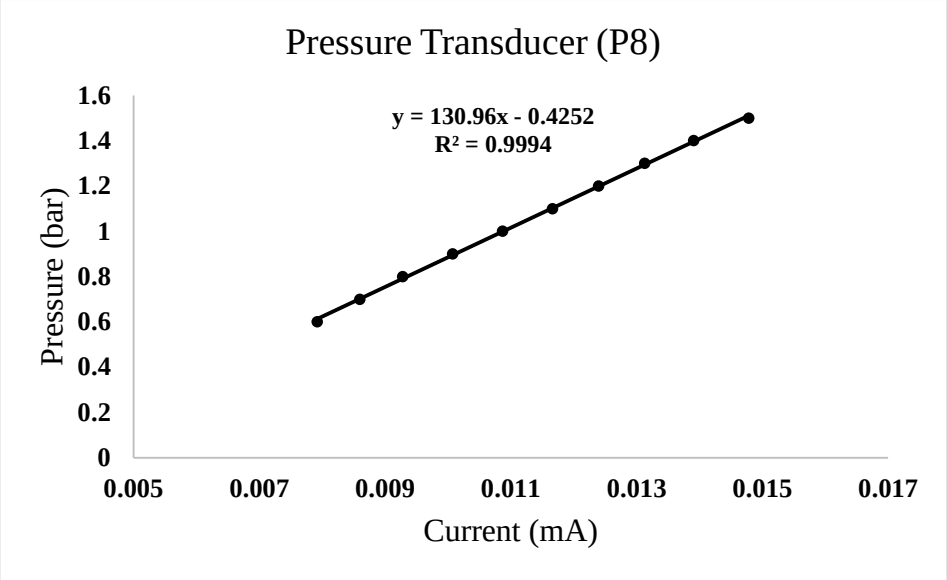

Figure 3.2: Regression analysis of calibration on pressure transducers (P2-P8)

3.5 Experimental Technique

In experiments, tests runs are performed by varying the starting pressure and volume flow rate of conveying air. Wypych (1989) also suggested following procedures, which were divided into three sections: pre-test procedure, testing method and post -test investigation (Ratnayke, 2005). In the pre-test procedure, setting of data acquisition system, software programming in acquisition system and setting of test rig is performed whereas post-test analysis is related to data analysis of the pressure readings. In post-test analysis, the steady state values of pressure are extracted from the raw data to check the pressure drop in the pipeline.

3.6 Testing Methodology

To carry out the extensive experiments with different powders in a pipeline, a test facility has been developed. During the experimental work a number of parameters must be recorded to do the further processing of experimental data. To manage all this, the following considerations were made during the development of this test setup;

- Testing was planned to be done on 50 mm I.D. x 70 m long pipeline.
- A 0.2 m^3 capacity blow tank was taken.
- To vary the conveying air pressure and mass flow rates of air valves were used.
- Testing was planned to be done on two materials (White cement and Grey cement).
- The parameters that need to be measured during the experiments were selected and to measure all these parameters provisions were made. Two set of load cells were installed to measure the

material discharge rate. Five pressure transducers were installed to measure the pressure at different desired locations. One flow meter was installed to measure the air flow rate.

- The different air flow rates, blow tank initial pressure, total pipeline pressure drop, pressure drop due to bends and m_s are the parameters that will be measured.
- PLC and pneumatic control panel were installed for the automatic actuation of the valves.
- Data acquisition system was used to record all the data. Data collection system records large number of readings per cycle, these data points is plotted with time and steady state data is obtained from the plots, which is used for further post-test analysis.

3.7 Experimental Results of PCC for White cement and Grey Cement

Steady state values of pressure are then used to draw PCC for different materials. In the present study, the experimental results of pressure drop for grey cement and white cement are used to draw PCC of the experimental data.

The results of pressure drop, mass flow rate of air and solid loading ratio, shows that the variation of solid flow rate for both the materials is very less(4.8t/h to 7.2 t/h) which clearly shows that PCC results will have a single constant solid flow rate line.

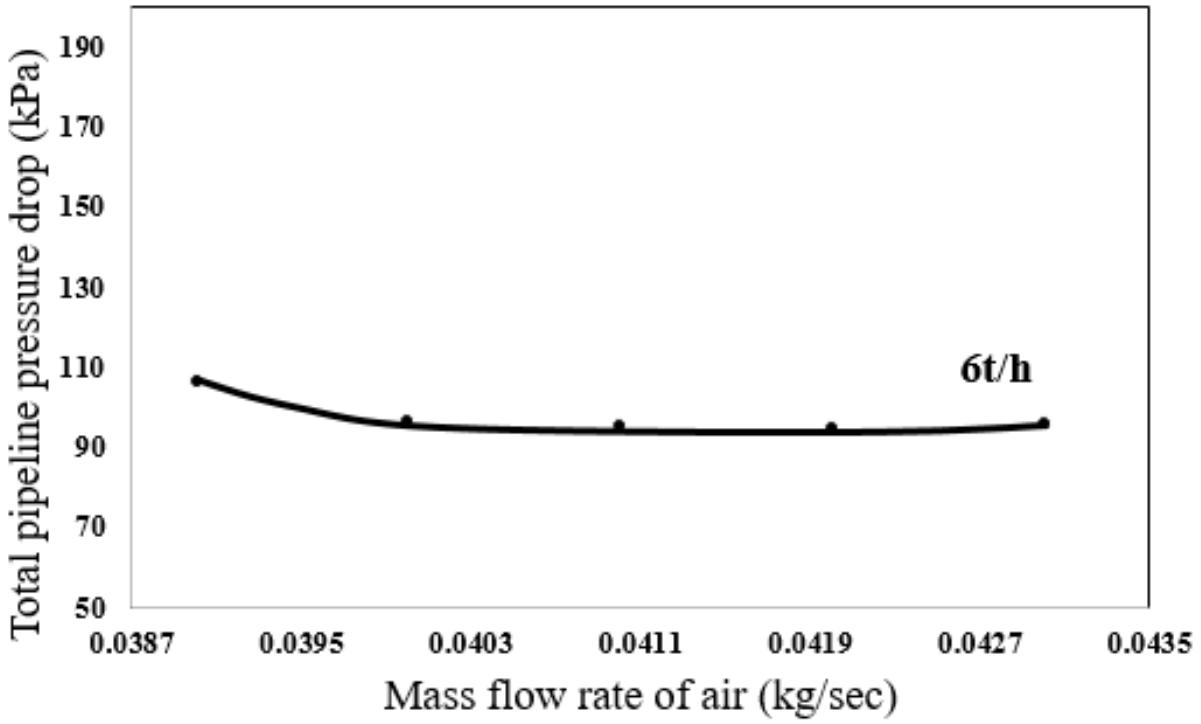

Figure 3.3: Experimental PCC for white cement 50mm I.D. × 69m test rig

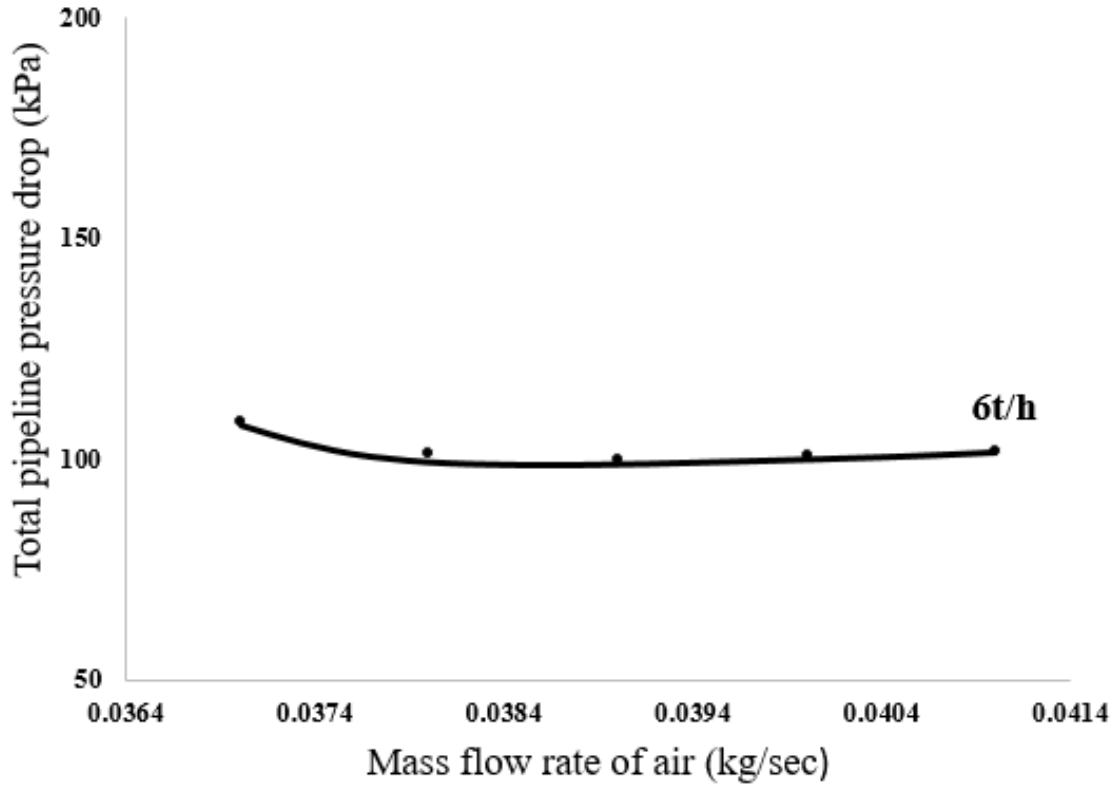

Figure 3.4: Experimental PCC for grey cement 50mm I.D. × 69m test rig

The results obtained for above PCC as given in Fig. 3.3 and 3.4 shows that the total pipeline pressure drop gradually decreases till mass flow rate of 0.0378kg/sec for white cement and 0.0384kg/sec for grey cement, after which the pressure drop shows a constant trend for both PCC. The single tonnage of solid line suggests that the variation of solid flow rate from the blow tank is almost constant and also for such small variation in mass flow rate of air, the trend of PCC for most of the air flow rate is generally linear. The slope of pressure drop with mass flow rate of air is less steep and hence flow transition from dense to dilute is not much seen in above experimental PCC results.

Chapter 4

Methodology for Simulation study

4.1 CFD Simulation of straight pipe for Pressure drop prediction

The study of pressure drop is very significant for gas-solid flow in pneumatic conveying system. It is required to find the pressure drop needed for flow of particles from one point of the conveying line to other. This is done with the help of pressure transducers, which brings electrical signals of pressure values between two points and that electrical signal in the form of current is converted to digital values of pressure with the help of data acquisition system which is finally calibrated to give experimental pressure drop between two points where pressure transducers were installed. The experimental pressure drop for every set of experiments is measured by pressure transducers as discussed above. But one of the objective of this thesis work deals with calculation of pressure drop through straight pipe with the help of CFD simulation and finally drawing plots for transition mechanisms i.e. PCC of the simulated pressure drop.

The summary of basic steps such as physical setup, types of solvers, boundary conditions for both phases, convergence criteria required to conduct the CFD study for predicting pressure drop is presented in subsequent section.

4.2 Numerical Simulation

The types of solver, models and other significant simulation steps are discussed in this section.

Solver: Pressure Solver was used for pressure correction derived from conservation of mass of incompressible flow. Steady state conditions were assumed.

Models: Eulerian multiphase model was used as the solid volume fraction was more than 10% for most of the cases and also the viscosity ratios of flyash and air are equal.

4.2.1 Boundary Conditions:

Selection of suitable boundary conditions is necessary for both phases and mixture at the inlet, outlet and wall of the pipe as mentioned in subsequent sub-sections:

At the inlet for mixture take initial absolute pressure same as experimental inlet pressure of pipe. For gas phase take uniform axial air velocity in m/sec. Again intensity of turbulence (5%)

and hydraulic diameter (inner pipe diameter) was used. No slip boundary condition was chosen at the wall. The outlet boundary condition was taken as pressure outlet.

Inlet is velocity inlet for the solid phase. An axial velocity (U_s)was chosen for the solid phase which was calculated with the formula given in Eq. (4.1)

$$U_s = \frac{m_s}{\rho_b \mathrm{A}} \tag{4.1}$$

For, the solid phase volume fraction was also defined for each set of simulation which was calculated as per the formula given in Eq. (4.2).

$$V_f = \frac{vs}{vs+va} \tag{4.2}$$

At the outlet, pressure was assumed to be zero. And all other flow variables were set to Neumann boundary conditions.

4.2.2 Experimental setup used for simulation

Geometry of the pipe was generated through inbuilt geometry modular of ANSYS FLUENT 15 software which was further used for meshing of a 3D straight pipe of length 6m and diameters (105mm ID and 68mm ID) respectively for the two different sets of simulation. The experimental test setup used for the simulation study are shown in Fig. 4.1 and 4.2. For this computational study the data obtained from P9-P10 transducers for the two test setups at Bulk Material Handling Lab, Australia by (Wypych et al., 2005) with flyash as the conveying materials having particle density (2300 kg/m^3) were used for the simulation of the straight pipe. The details of the experimental setup of University of Wollongong is given below:

1) It consist of two blow tanks each having capacity of 0.5m^3.
2) A receiver bin with installed capacity of 6m^3 and pulse jet bag filter was used to store materials.
3) In this study simulation tests were performed on two setups 69 mm I.D. × 168 m long, 105 mm I.D. ×168 m.
4) A rotary screw compressor (Model: P375-WP) supplied compressed air having maximum pressure of 800kPa and 10.6 m^3/min free air delivery
5) For this study pressure transducers (P9-P10) results were used for the simulation. Specification of Pressure transducers (Manufacturer: Endress and Hauser, Model: Cerabar PMC133, pressure range: 6 -2 bar, maximum pressure range: 40 bar (absolute), current signal: 4-20 mA.

6) Other instruments such as pressure reducing valve, blow valve. Load cells (Shear beam type) flow meters with standard calibration methods were used.
7) A portable Data logger with 24 channel connections was used to record data from load cells, flow meter and pressure transducers.

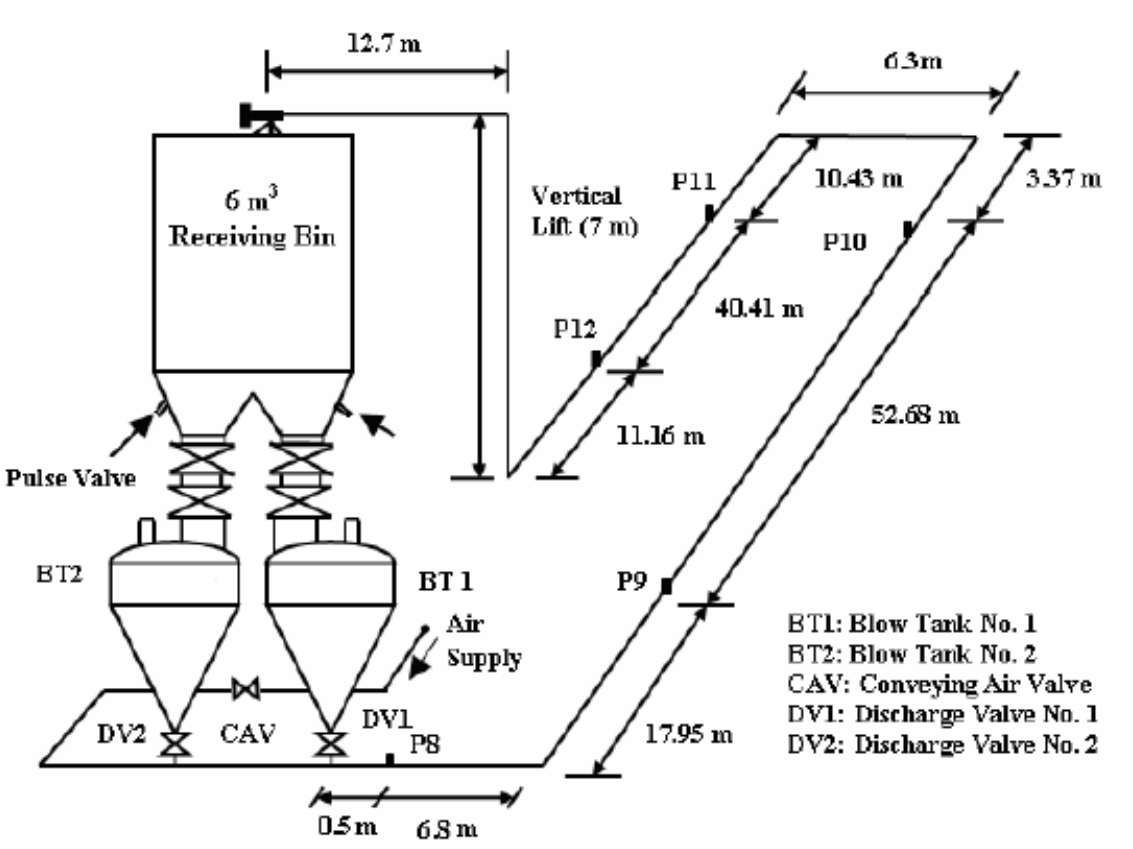

Figure 4.1: Layout of the 69mm I.D.×168m test rig for flyash

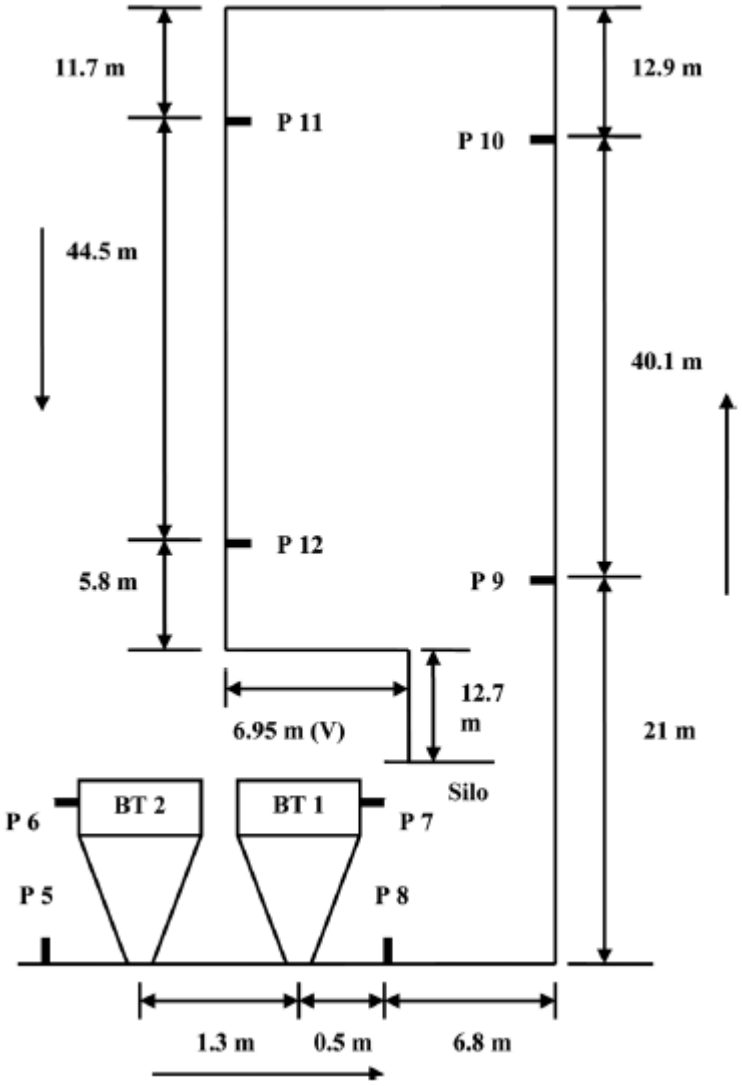

Figure 4.2: Layout of 105mm I.D. ×168m test rig for flyash

4.2.3 Solution Approach and Convergence

Calculations in multiphase flow needs appropriate strategy to avoid divergent solution. A second order upwind method is generally used to solve momentum equations and the QUICK (Quadratic Upstream Interpolation for Convective Kinetics) scheme is mainly used for solid volume fraction. A First order Upwind Scheme is used for Granular Temperature, Turbulent kinetic energy and Turbulent Energy dissipation rate. These schemes are generally used to assure reliability of solution and achieve faster convergence results. The convergence criteria is based on the residual values of the flow variables such as momentum, continuity, kinetic energy, epsilon, and volume fraction of solid. The solution is expected to be converged when all the normalized residuals falls below a stipulated absolute convergence criteria. In this simulation study the residual values of all flow variables are assigned value of 10e-^{6} for better

convergence results. The simulations are carried out at steady state run of 5000 iterations. A convergence result of the scaled residuals from one of the simulation is shown in Fig. 4.3. As can be seen from the given figure the flow variables such as continuity, velocities of each phase in x, y, z direction, volume fraction, kinetic energy and epsilon which is turbulent dissipation all are converged before 3500 iterations.

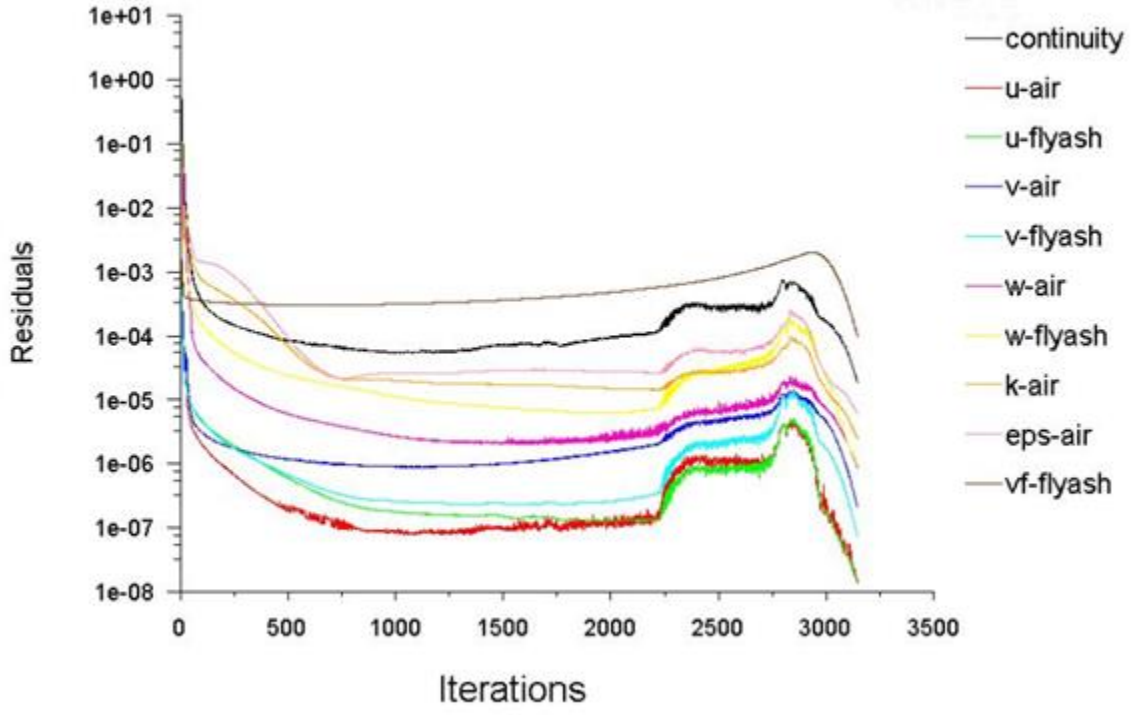

Figure 4.3: Convergence result of the scaled residuals

4.3 Pipe Geometry and Meshing

The pipe geometry used for this study, is a 3D circular straight pipe of diameters (105mm ID and 69mm ID) having length of 6m for two different sets of simulation with respective inlet, wall and outlet as shown in Fig. 4.4

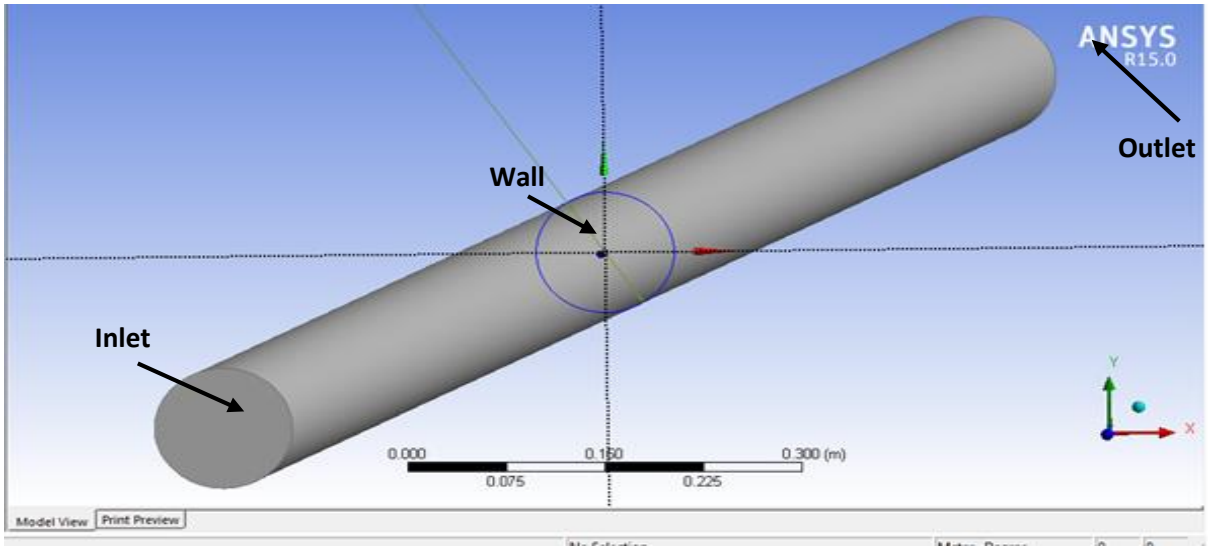

Figure 4.4: Geometry of 3D Straight Circular Pipe

Table 4.1 shows the simulation factors and the standards which were used in this study for calculation of pressure drop. These factors need to be selected carefully as they are also one of the key parameters that affects the end results.

Table 4.1: Simulation Factors

Factors	**Standards**
Solver Type	Pressure Based
Velocity Formulation	Absolute
Time	Steady
Multiphase	Eulerian
Turbulent model	Realizable k-ε model
Near wall Treatment	Standard wall function
Turbulent Multiphase model	Dispersed
Pressure Velocity Coupling	Phase Coupled Simple
Turbulent Intensity,%	5
Roughness Constant	0.5
Hydraulic diameter, m	Equals to pipe diameter
Operating Temperature, K	293
Granular Temperature, m^2/s^2	0.0001

Grid generated after meshing is shown in Fig. 4.5. Meshing was generated using Sweep selecting the element size of the sweep for one of the face equal to 20cm. The inlet, outlet and wall were named as the actual pipe inlet and exit and the surface of the pipe was selected as the wall. The elements of the mesh were 285000 and the nodes were 315105 respectively. All the three parameters which define a good quality mesh were satisfied i.e. Aspect ratio was within 5, Orthogonality was equal to 0.99 which should be close to 1 and the Skewness was 0.56 and it should be less than 1.

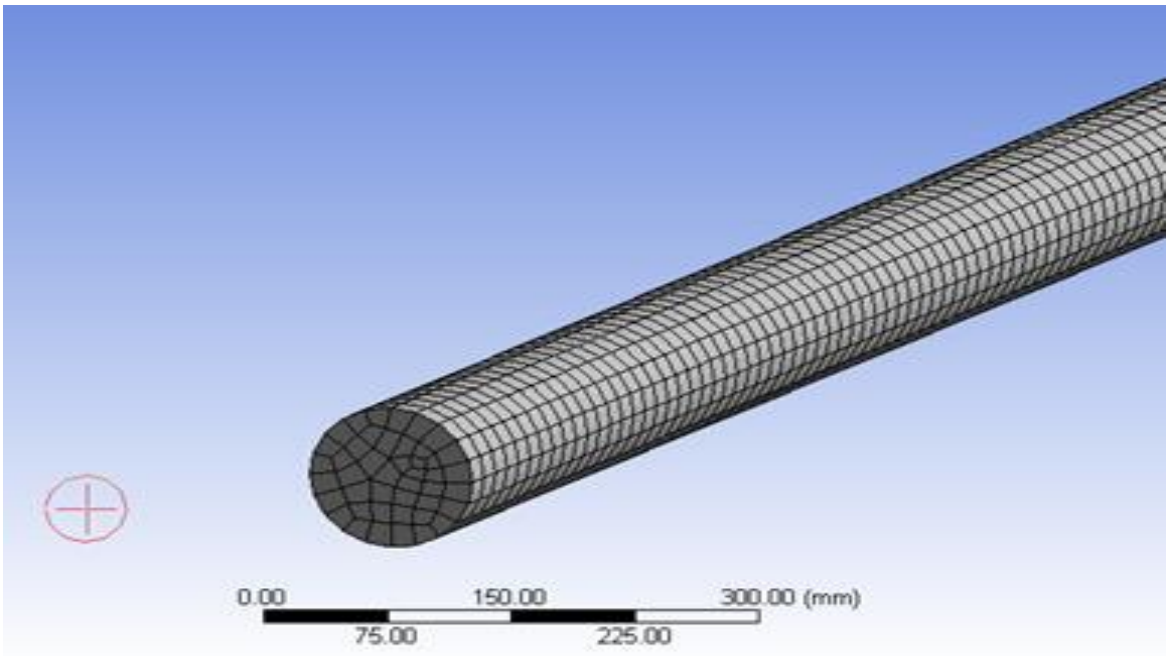

Figure 4.5: 3D Computational Grid

The volume and area statistics values should be positive for good quality mesh. The statistics of the above generated mesh is presented below:

Volume Statistics:

Minimum Volume (m^3): 1.396877e-9

Maximum Volume (m^3): 1.223802e-6

Total Volume (m^3): 4.413621e-2

Face area Statistics:

Minimum face area (m^2): 1.290811e-6

Maximum face area (m^2): 1.366987e-4

4.4 Grid Independence study

It is mandatory to perform the grid independence study as the results are highly dependent on the quality of grid. So grid independence test is performed to make the results independent of the grid size. The general philosophy of better results from simulation is to refine the mesh into smaller control volumes, but this in turn leads to longer computation time. After conducting grid independence test there is no need to further refine the mesh for better results. In this study,

grid independence test was performed on both pipe geometries (69mm I.D. ×6m), (105mm I.D. ×6m) straight pipe. For 1st pipe the grid was sized to different element sizes of (15mm, 12mm, 10mm, 8mm and 7mm). The results of pressure drop obtained were almost similar for mesh size of 15mm and 7mm, having pressure drop equal to (1.7721kPa and 1.7578kPa) respectively. Thus all 27 simulation for pipe (69mm I.D. × 6m) were performed on meshed pipe of grid size 15mm.

For pipe with configuration (105mm I.D. ×6m), the grid independence test was performed with grid size of (7mm, 9mm, 10mm, 11mm, 12mm and 15mm). The results of pressure drop obtained were almost closer for grid size of (15mm and 11mm) having values of (1.7271kPa and 1.7547kPa) respectively. Thus all 25 simulations for pipe (105mm I.D. ×6m) were performed on meshed pipe of grid size 11mm.

For each sets of simulation point the inlet pressure was given equal to experimental value of pressure given by P9 transducer, the mean particle diameter (d_{50}): 30μm was used as the particle diameter, the inlet velocities of air and flyash was also given, the particle density: 2300kg/m^3 and bulk density: 700kg/m^3 was used for all the simulation points. The volume fraction of each set of simulation was given as per the calculation from equation 3. Outlet pressure was assumed to be zero. As already discussed, the convergence criteria of flow variables was taken equal to 10e-^{6}. The number of iterations for calculations were taken to be 5000.

Chapter 5

Results & Discussions

5.1 Computational Investigation of pressure drop through CFD

The simulation results of pressure drop obtained are compared with experimental values which are further used to draw PCC for both experimental and simulation pressure drop per unit length with the help of interpolation relationship technique (Mallick, 2010). The simulation tool was also used to study the significant effects of various factors like particle diameter, density and volume fraction on the pressure drop.

The results of post processing in the form of pressure drop was calculated for each simulation data points considered in this study. For each pipe geometries of 69mm I.D. × 6m and 105mm I.D. ×6m straight pipes, the comparison of experimental and simulated values of pressure drop per unit length are given in Table 5.1 and 5.2.

5.2 Simulation results for 69mm I.D. × 6m pipe and comparison with experimental data

From Table 5.1 it can be observed that the average deviation in the percentage error of experimental & simulated pressure drop per unit length was found to be 20% while for few cases it was close to 25 to 28 %. Volume fraction of flyash may be one of the reason for this change in pressure drop, as higher is the solid volume fraction more pressure drop can be noticed. Also for all these 27 simulation points volume fraction is different as flow varies from dense to dilute phase, which clearly maybe one of the reason for this deviation in pressure drop.

Table 5.1: Simulation results for 69mm I.D. × 6m straight pipe

Experimental pressure drop per unit length (Pa/m) (P_{actual})	**Simulation Pressure drop per unit length(Pa/m) ($P_{predicted}$)**	**(P_{actual}- $P_{predicted}$/ P_{actual})×100 (%)**
491.3	397.6333	19.0651
425.615	315.75	25.81327
434.033	326.4833	24.77914
467.863	397.5783	15.02256
503.415	429.56	14.67083
524.053	427.9667	18.33523

530.854	414.2767	21.9604
531.32	416.575	21.59621
561.249	479.2083	14.61754
698.302	531.2833	23.91779
740.501	590.7667	20.22064
554.219	444.3017	19.83276
587.85	464.5233	20.97924
607.456	475.385	21.7417
633.24	469.02	25.93334
647.131	483.2417	25.32553
650.373	485.43	25.36134
695.77	521.3217	25.07265
769.31	594.72	22.69436
667.983	502.793	24.7297
728.145	569.975	21.72237
725.8146	565.4267	22.09764
753.5	596.6317	20.81863
767.0865	613.4267	20.03161
821.7753	664.2983	19.16302
838.554	683.9733	18.43421
421.953	303.065	28.17566

The comparison of the experimental & simulated pressure drop per unit length for 69mm I.D. ×6m straight pipe given in Fig. 5.1 shows that the average % error in pressure drop was 21.55% and the standard deviation error was equal to 3.55%, which shows really a good trend as per the simulation results of CFD. The undeprediction of simulation results of pressure drop may be because of inbuilt software codes used for the simulation study, which can be changed to some user defined codes as per the requirement of the study for better prediction of pressure drop.

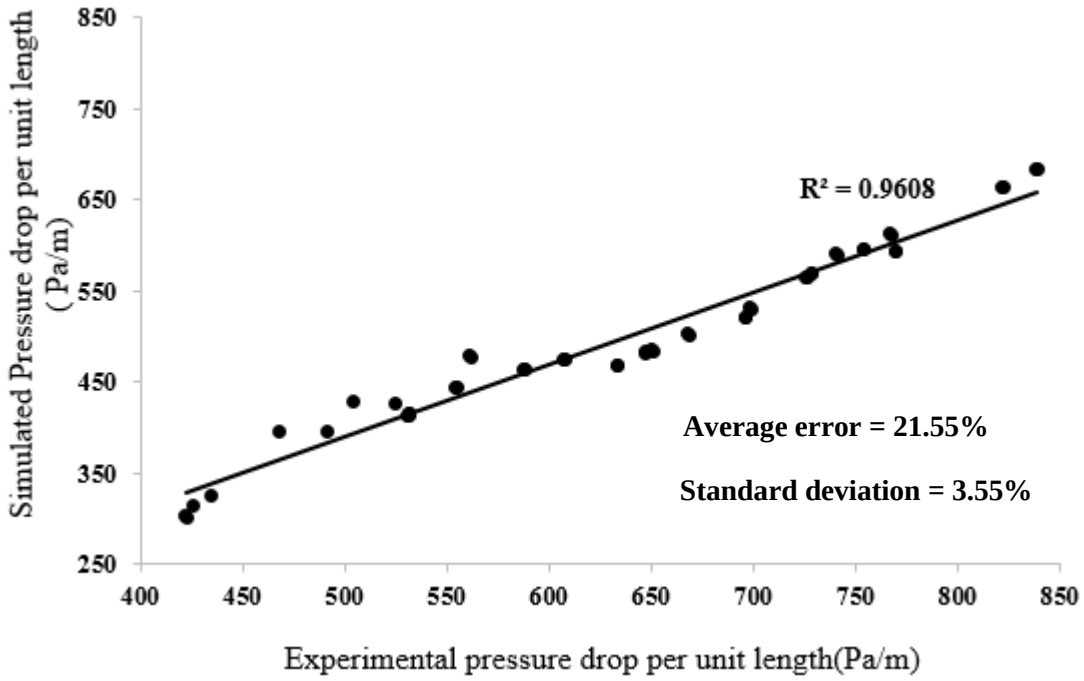

Figure 5.1: Comparison of Experimental (69mm I.D. ×168m) and simulated pressure gradient

.

5.3 Simulation results for 105mm I.D. × 6m and comparison with experimental data

Simulation results of pressure drop for 105mm I.D. ×6m straight pipe for 25 sets of data points as can be noticed from the Table 5.2 shows that the maximum percentage error was 30.57% but it also reached minimum to 5.32%. The reason for this variation may be because of variable volume fraction, as change in volume fraction have an appreciable effect on pressure drop which is explained in the subsequent section of this chapter.

Table 5.2: Simulation results of 105mm I.D. × 6m straight pipe

Experimental pressure drop per unit length(Pa/m) P_{actual}	**Simulation Pressure drop per unit length(Pa/m)** $P_{predicted}$	$(P_{actual-} P_{predicted/} P_{actual)\times 100}$ **(%)**
314.2145	287.945	8.360361
321.6958	285.321	11.3075
339.1521	321.0767	5.3296
339.1521	320.8943	5.624453
359.1022	336.7033	6.237475
359.1022	336.5383	6.283422

314.2145	288.3567	8.229347
364.0898	334.975	7.996592
389.0274	364.521	6.299667
246.8828	171.3933	30.57704
251.8703	179.7083	28.65045
259.3516	183.7321	28.00122
246.8828	174.6633	29.25253
271.8204	204.9267	24.60955
274.3142	208.2215	24.09435
281.7955	216.4417	23.19194
289.2768	224.2083	22.4935
286.783	222.2833	22.49077
301.7456	250.945	16.83558
316.7082	270.116	14.7114
341.6459	288.365	15.59535
403.99	361.2736	10.57363
331.6708	276.49	16.63723
336.6584	273.0917	18.88166
451.3716	420.3215	6.879381

The average percentage error in pressure drop was found to be 15.96% and the percentage standard deviation error was 8.66% which shows really good trends as per the simulation capability of the software. The overall comparison of the pressure drop of experimental and predicted results can be seen in Fig. 5.2, which clearly shows some under prediction of simulation pressure drop. This maybe because of inbuilt software codes used for pressure drop calculation which obviously have some limitations. Better results can be achieved if some user defined codes are used for prediction of pressure drop.

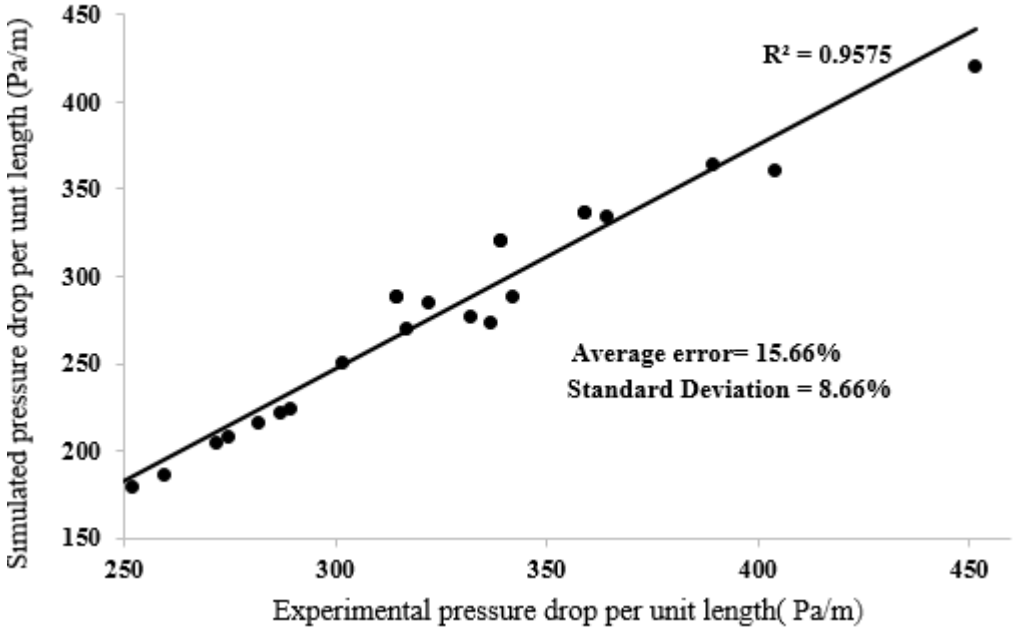

Figure 5.2: Comparison of Experimental (105mm I.D. ×168m) and simulated pressure gradient

From the above results of comparison of pressure drop per unit length of experimental and simulated pressure drop, the data points of pressure were interpolated to generate the PCC, which is a graph between pressure drop per unit length on Y axis and the mass flow rate of air (kg/sec) on X axis at specified solid tonnage(t/h).

5.4 Method to Plot PCC

As we know that in Pneumatic Conveying, PCC Curve are the plot of the pressure drop per unit length on Y axis and mass flow rate of air on X axis for varying solid flow rates(t/h). Final PCC from simulation data points are drawn by using an interpolation relationship technique (Mallick, 2010). In this technique, the experimental data points are plotted as shown in Fig. A.3 and A.4 of Appendix A. These experimental data points are the PCC data points for the P9-P10 transducers shown in the setup given in Fig. 4.1 and 4.2. These experimental data points may not be for constant solid flow rate lines because even though we try to maintain a constant solid flow rate through blow tank, it's technically impossible as the solid flow rate varies for every test run. Interpolation technique is used with m_a and ΔP_t values of data points which are close to each other up/down (vertically) along a specific value m_s to get the intermediate data points. Suppose we have to find intermediate pressure value and mass flow rate of air value from Fig.

A.1 of Appendix A. Let's select the points 13 and 3to find the intermediate point say 4 having 9t/h as the mass flow rate of solid. Then the expressions given in Eqs. 5.1 and 5.2 (Mallick, 2010) were used to find the intermediate data points.

$$\frac{\Delta P_4 - \Delta P_3}{m_{s4} - m_{s3}} = \frac{\Delta P_{13} - \Delta P_3}{m_{s13} - m_{s3}} \quad (5.1)$$

$$\frac{mf_4 - mf_3}{m_{s4} - m_{s3}} = \frac{mf_{13} - mf_3}{m_{s13} - m_{s3}} \quad (5.2)$$

With the help of these equations, the values of ΔP_4 and m_{a4} are determined at specified value of solid flow rate. Similarly through this interpolation technique other intermediate points were calculated. In order to find the constant solid flow rates lines, the points which were vertically downwards were selected for interpolation. Also the far away points were not selected in order to avoid errors. If the intermediate points follow clear trend of PCC then we need to obtain a best fit curve manually with the help of hand passing through the intermediate data points.

The experimental and simulation data points on PCC are given in Fig. A.1 to A.4 of Appendix A. These data points were interpolated to give intermediate data points for PCC which were then plotted with a best fit curve to give the final PCC of the experimental and simulated data.

5.5 Experimental PCC of flyash 69mm I.D. × 168m straight pipe

The experimental results of PCC of 69mm I.D. ×168m as given in Fig. 5.3 shows that the flow transition from dense phase is gradual for all solid flow rate lines having pressure minimum around 0.07 kg/sec of air flow rate. The PCC result shows that the trend of pressure drop per unit length first decreases rather rapidly, and then the change of slope becomes low, leading towards change in trend. The trend lines changes from constant slope to increasing slope after air flow rate of 0.1kg/sec, which clearly shows that flow is about to enter dilute phase.

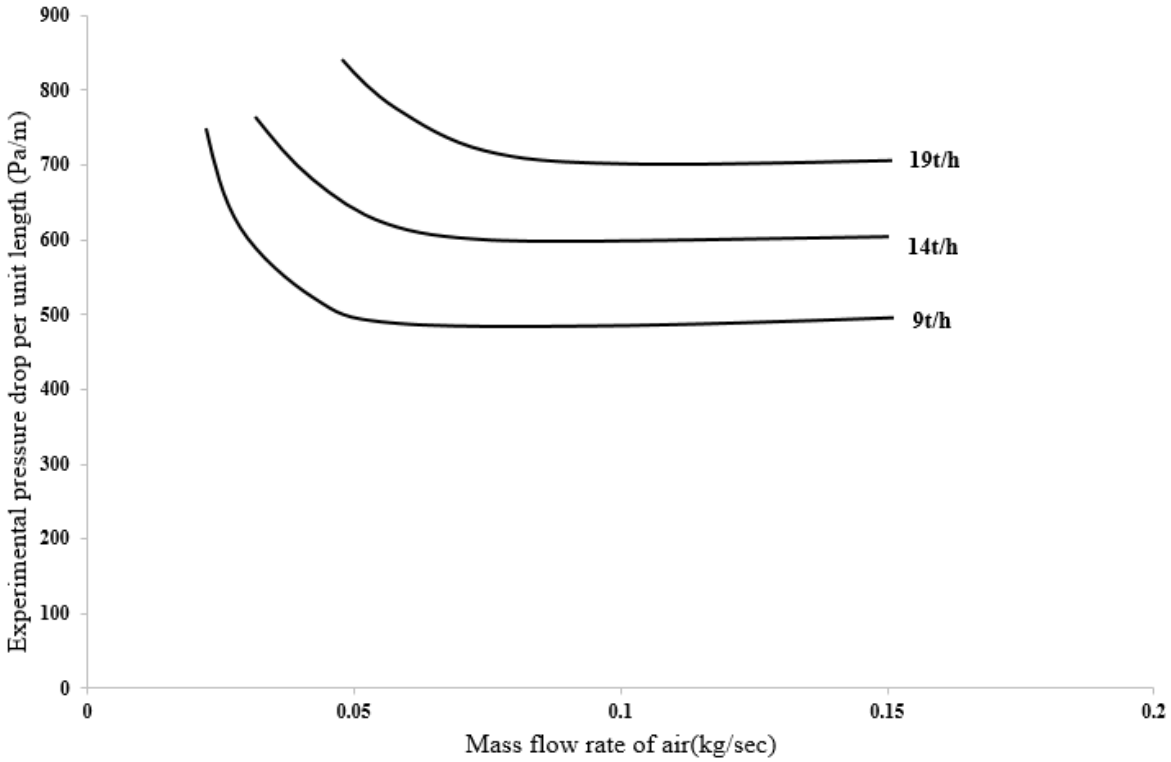

Figure 5.3: Experimental PCC of 69mm I.D. × 168m straight pipe

5.6 Simulation PCC of 69 mm I.D. ×6m straight pipe

The simulation results of PCC (Fig. 5.4) shows exactly the same trends of experimental PCC showing that the predicted values of pressure drop are really good to explain the flow mechanisms in pneumatic conveying. As can be noticed from above figure the slope of pressure drop per unit length for each different solid flow rate lines shows a sharp decreasing trend till 0.06kg/sec of air flow rate, after which slope of trend line almost becomes constant contrary to experimental PCC which shows increasing slope after some values of air flow rates. The reason for this little deviation of the two PCC curves is may be because of the difference in pressure drop whose average value of percentage error is 21.55%.

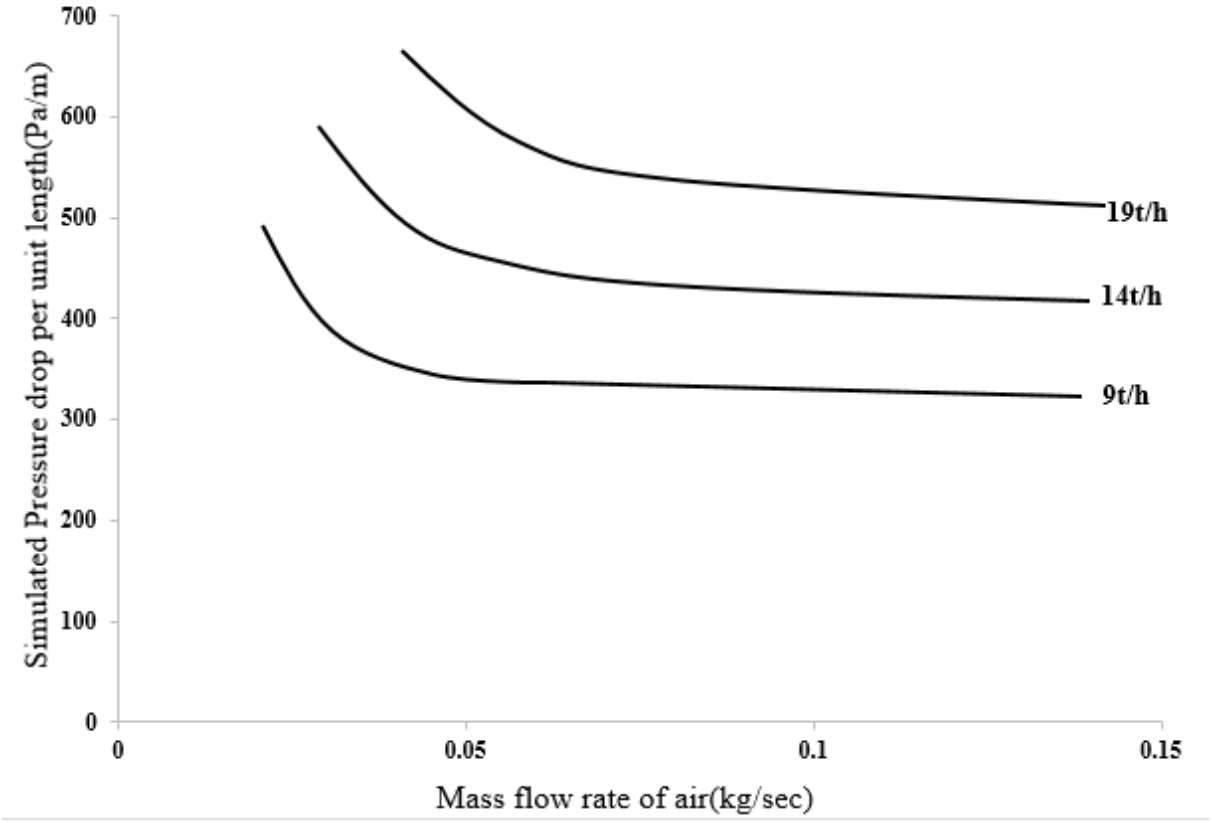

Figure 5.4: PCC for simulation of 69 mm I.D. × 6m straight pipe

5.7 Comparison of Experimental PCC of 69 mm I.D. ×168m and simulation PCC

Figure 5.5 shows a significant change in slope of PCC with increasing air flow rates. From 0.04kg/sec to 0.08kg/sec of air flow rate, pressure drop decreases with increase in mass flow rates of air. From 0.09kg/sec to 0.12kg/sec of air flow rates of experimental PCC shows a noticeable upward trend (i.e., pressure drop starts to increase with increasing air flow rates). While simulation PCC becomes almost horizontal (i.e., no appreciable change in pressure gradient even with increasing air flow) from air flow rates of 0.1kg/sec to 0.18kg/sec. The different shapes of experimental and simulation PCC suggests that there could be changes in flow mechanism along the flow direction (flow changing from dense-to-dilute phase along the flow direction).

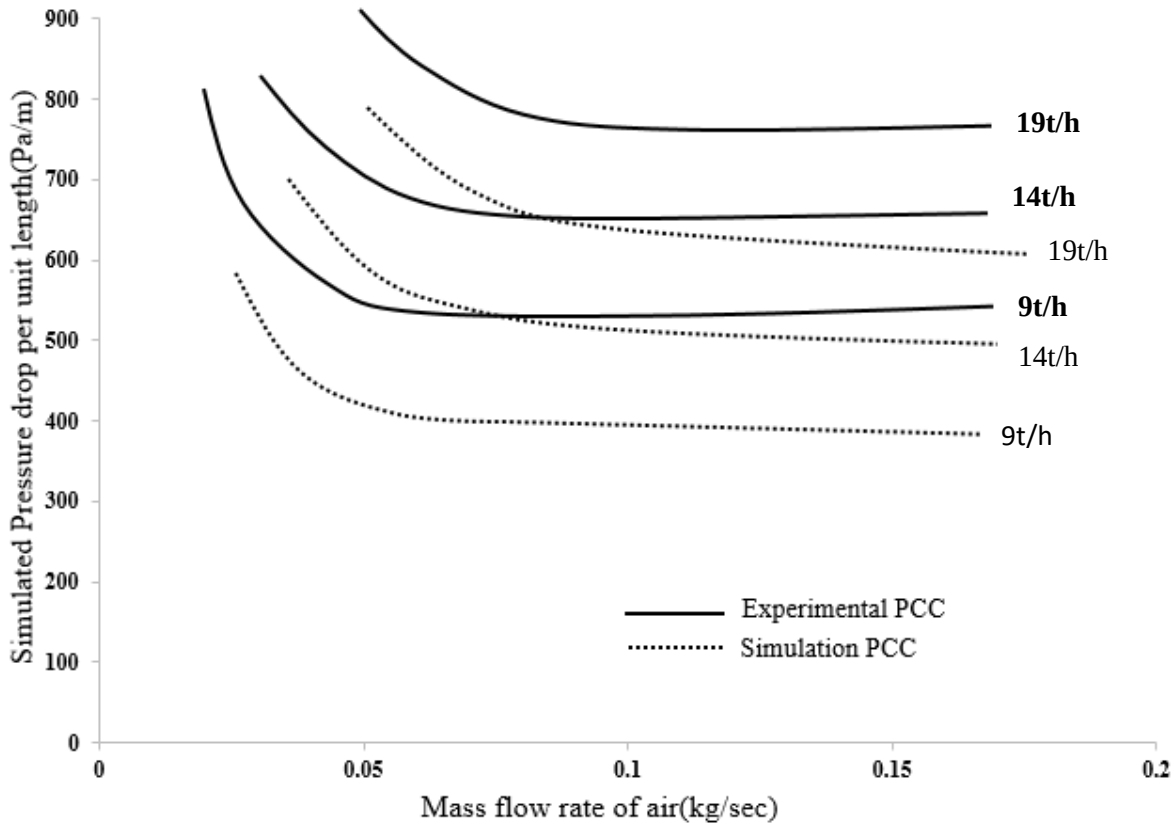

Figure 5.5: Comparison of Experimental PCC of 69mm I.D. ×168m vs Simulation PCC

5.8 Experimental PCC of 105mm I.D. ×168m straight pipe

The slopes of the trends in the pressure drop per unit length for the experimental PCC of 105mm I.D. × 168m as shown in Fig. 5.6, is almost identical for the three solid lines of 18t/h, 23t/h & 28t/h except the gradual decrease in pressure gradient is observed till air flow rate of 0.12kg/sec and after that the variation of pressure drop per unit length becomes constant.

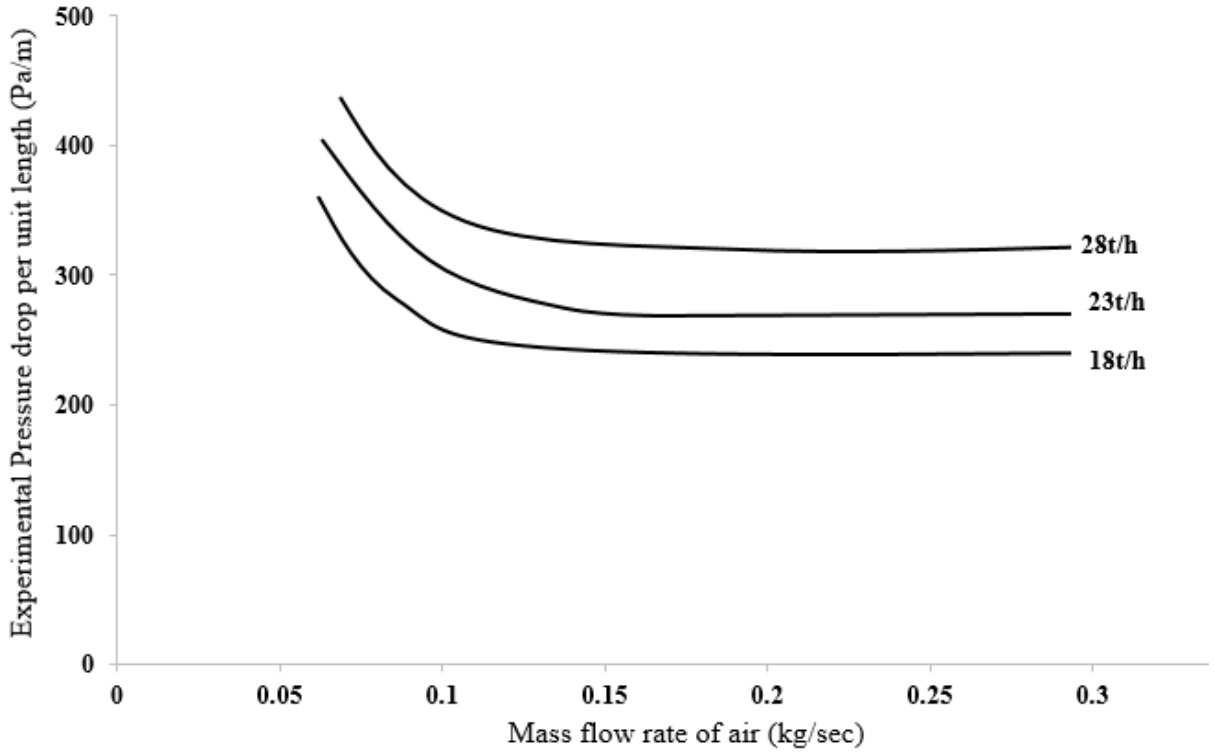

Figure 5.6: Experimental PCC of 105mm I.D. ×168m straight pipe

5.9 Simulation PCC of 105mm I.D. × 6m straight pipe

The PCC results of simulation as given in Fig. 5.7 are almost identical with experimental PCC except the fact that the constant trend in the pressure gradient is observed after air flow rate of 0.15kg/sec until that there is gradual steep decrease in the pressure drop per unit length with air flow rate. Also the slopes of trend lines are almost the same owing to less average error of pressure drop which is just 15.66%.

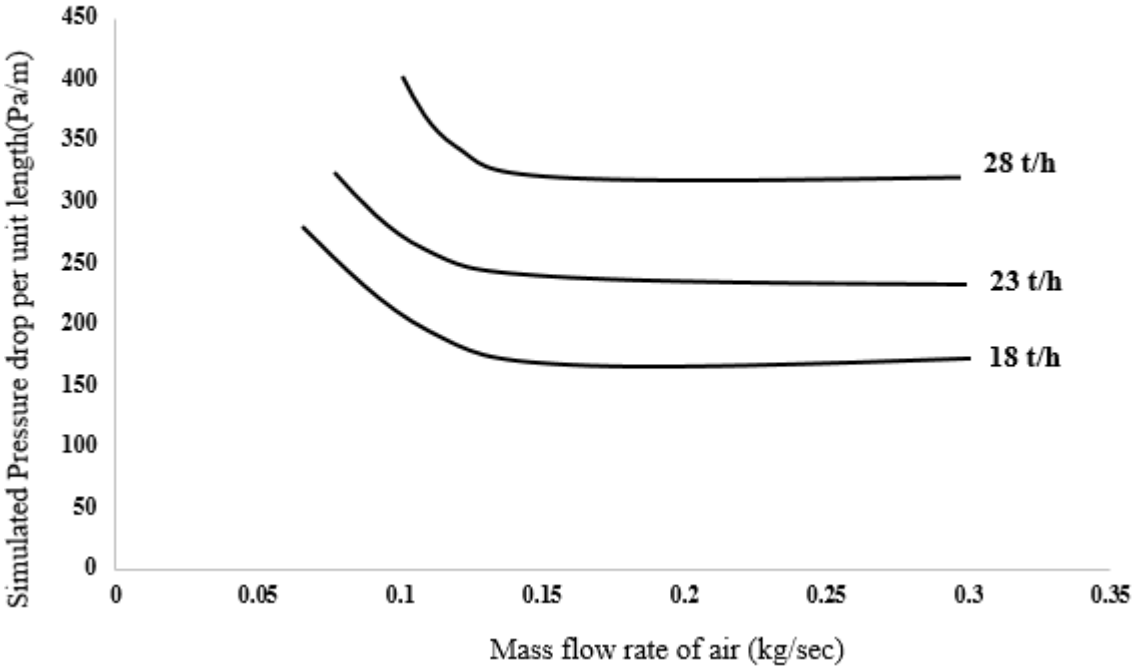

Figure 5.7: Simulation PCC of flyash (105mm I.D.× 6m)

Thus from above results of the PCC of simulation data points we observe that the trends in PCC are almost identical with the experimental PCC and hence CFD prediction of pressure drop is quite good and can be used for simulation of pneumatic conveying system to calculate the pressure drop and further using the values of pressure drop to plot PCC and compare it with experimental PCC curves. CFD simulation tool is also used to study the influence of particle diameter, density and volume fraction of flyash on the pressure drop.

5.10 Comparison of Experimental PCC of 105 mm I.D. ×168m and simulation PCC

Figure 5.8 shows that none of the PCC shows sharp change in slope. Experimental PCC shows gradually decreasing slope (only minor change in slope) at air flow rate of 0.08kg/sec, while simulation PCC shows air flow rate of 0.12kg/sec. After these air flow rates both PCC almost shows the same trend. The change in slope may be an indication of change in flow characteristics in the flow direction. However, there was no distinct PMC in either set of PCC, indicating that even if there were a flow transition, the change is gradual. Experimental PCC provides higher pressure gradient than simulation PCC.

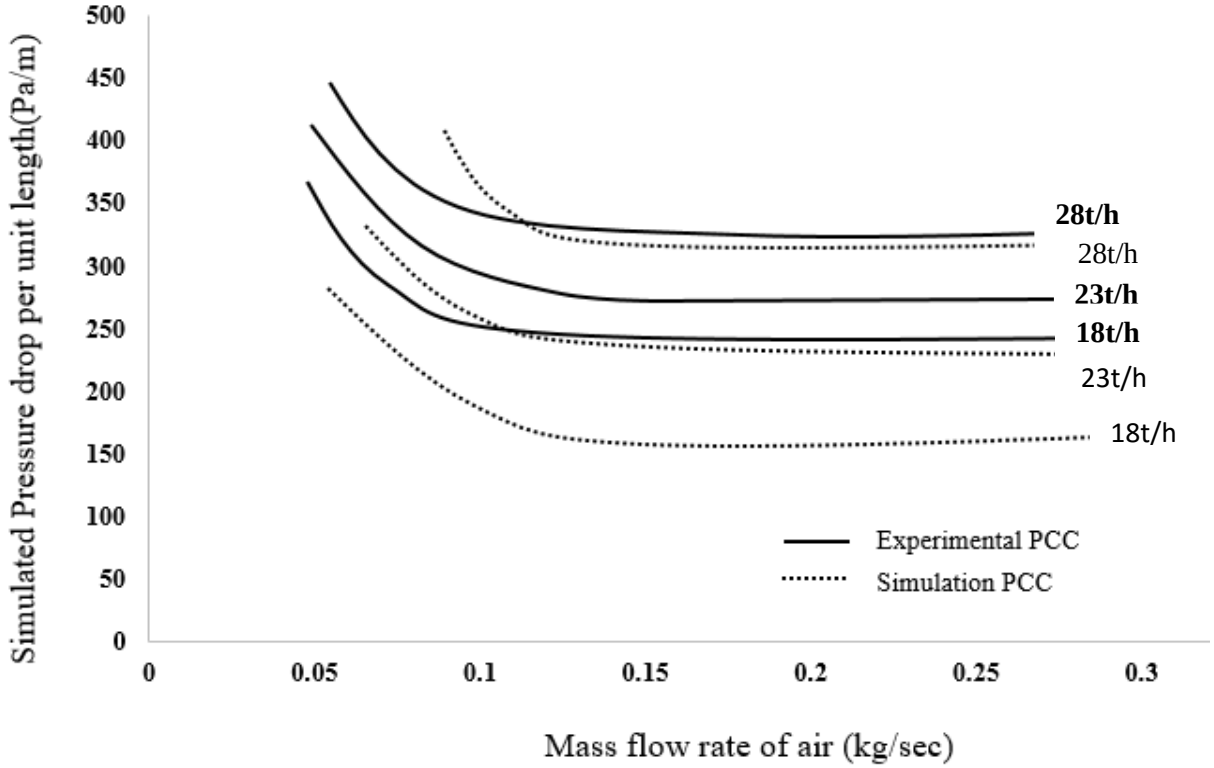

Figure 5.8: Comparison of Experimental PCC (105mm I.D. ×168m) vs Simulation PCC

5.11 Effect of particle diameter on the pressure drop

The effect of particle diameter on the pressure drop keeping all other parameters constant is shown in Fig. 5.9. The different particles used are 19µm, 30µm, 60µm, 100µm, 150µm supposing the particles to be of spherical shape. The pressure drop was calculated for these diameter values at different solid volume fraction. The superficial gas velocity used was 17.52m/sec. It can be observed that pressure drop first increases, reaches peak value around mean particle diameter of 30µm and then it starts decreasing. The reason for the sharp increase in pressure drop at mean particle diameter is because of increase in drag force around the peak diameter of particle but after that the drag force between particles dominates and hence after peak particle diameter pressure drop decreases with increasing particle diameter.

The same effect is observed at different solid volume fraction, higher is the solid volume fraction more increase of pressure drop can be noticed.

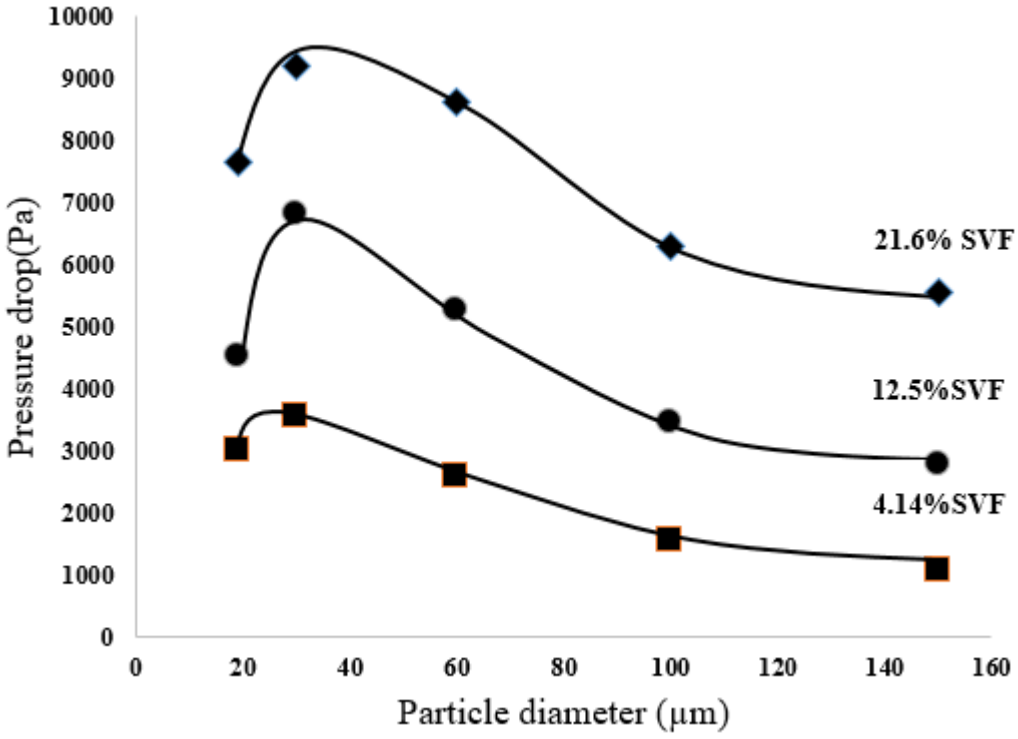

Figure 5.9: Effect of particle diameter on the pressure drop at different values of solid volume fraction

5.12 Effect of Particle density on pressure drop

It can be analysed from Fig. 5.10 that increase in particle density leads to increase in pressure drop. The reason for this change is the necessity of high energy to transport heavy particles at higher density. The results for pressure drop with particle density at different particle diameter (19µm, 30µm and 60µm) shows almost similar increasing trend although more increase in pressure drop with varying density was found for large diameter particle.

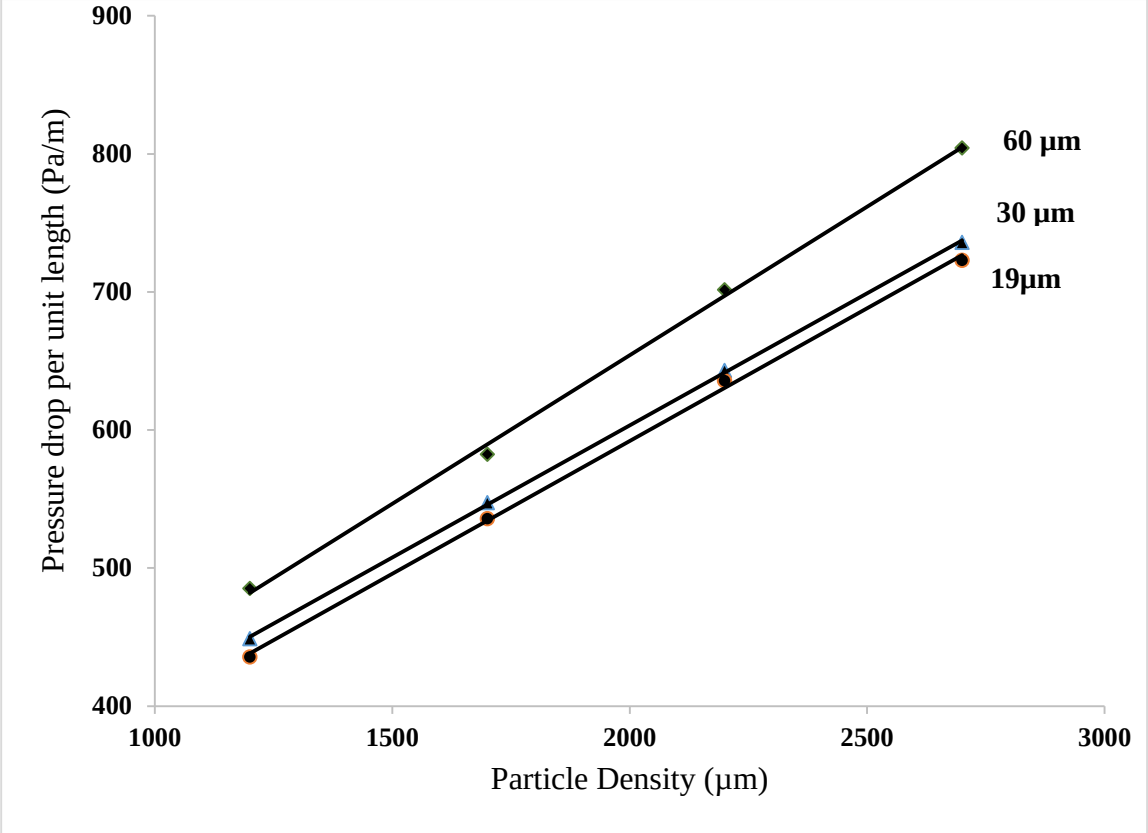

Figure 5.10: Effect of particle density on the pressure gradient for different particle diameter

5.13 Effect of Volume fraction on pressure drop

The results of the effect of volume fraction on the pressure drop are shown in Fig. 5.11. It shows that pressure drop increases linearly with volume fraction of solid. For different values of particle densities (700kg/m^3, 1200kg/m^3, 1700kg/m^3), the effect of varying the particle volume fraction 4.14%, 6.25%, 8.42%, 10.24% and 12.72% is studied on the pressure drop in straight pipe. The increase of pressure drop with solid volume fraction, is mainly due to the reason that air velocity gets reduced on increasing volume fraction of solid which ultimately leads to decrease in the slip velocity between particle and air and results in overall increase of pressure drop.

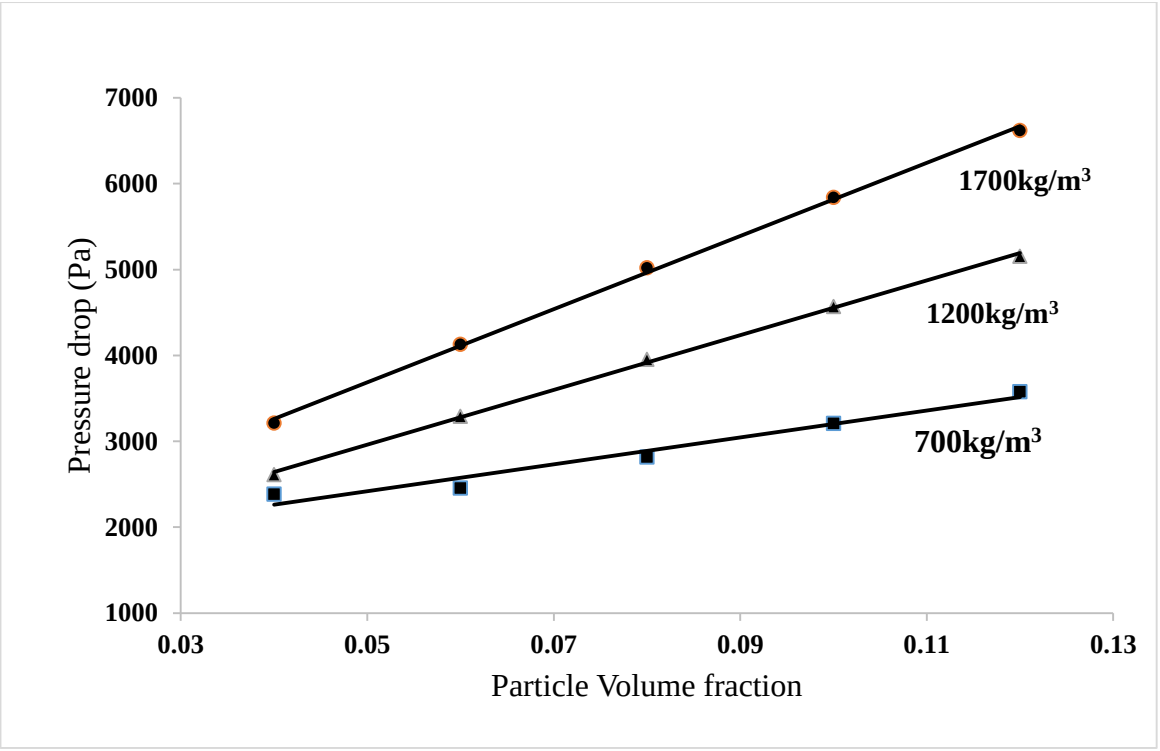

Figure 5.11: Effect of volume fraction on pressure drop at different particle density

5.14 Results of contours of volume fraction of flyash at different particle diameter

The results of contours of flyash at different particle diameter as given in Fig. 5.12 suggests that as particle diameter increases the solid concentration at the bottom of the pipe also increases. Also the maximum volume fraction of flyash at particle diameters of (19µm and 30µm) is 12.7% which is less than particle volume fraction for large diameter particles of flyash (60µm and 100µm). High solid volume fraction at the bottom of the pipe with increasing particle diameter suggests that coarser particle settles at the bottom due to less cohesive forces between the particles.

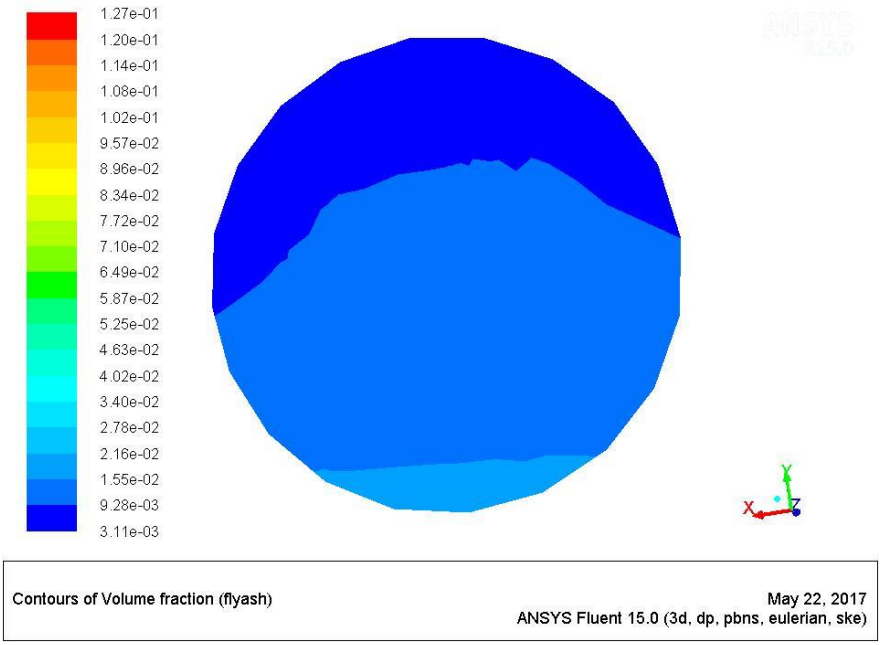

Solid volume fraction (19µm)

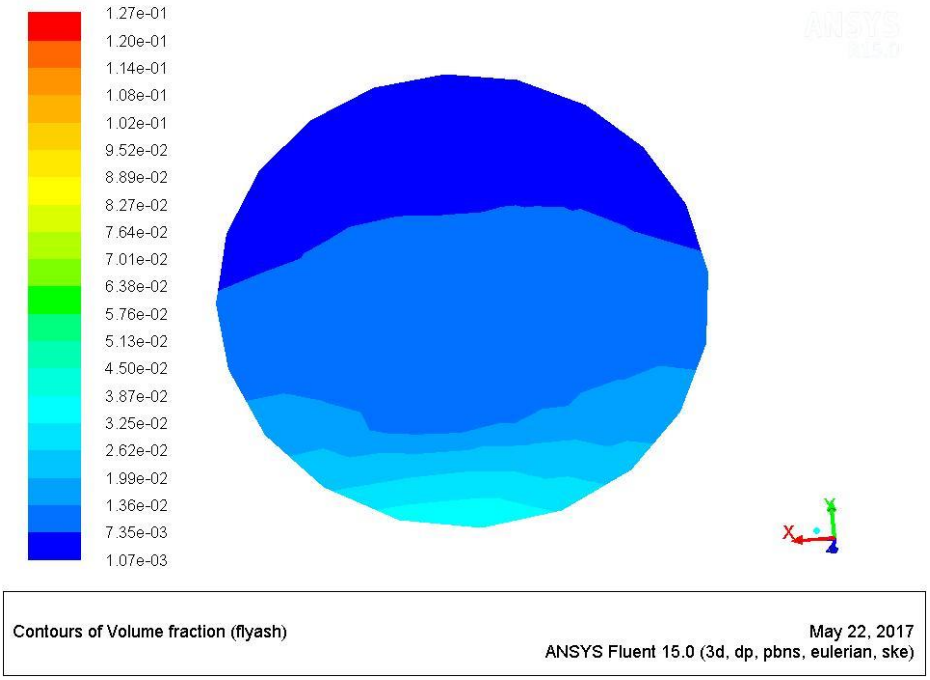

Solid volume fraction (30µm)

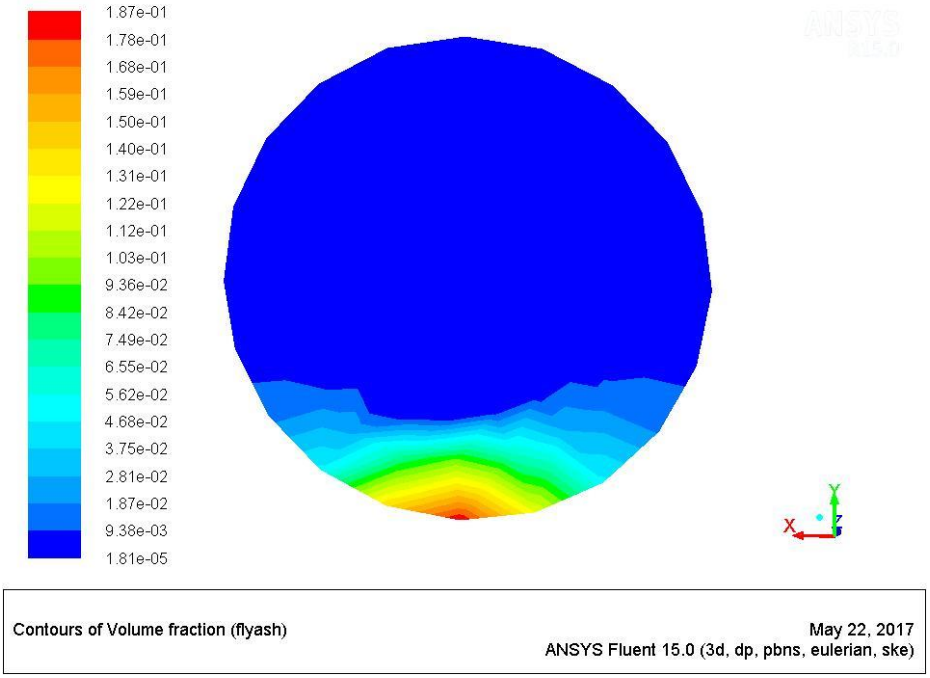

Solid volume fraction (60µm)

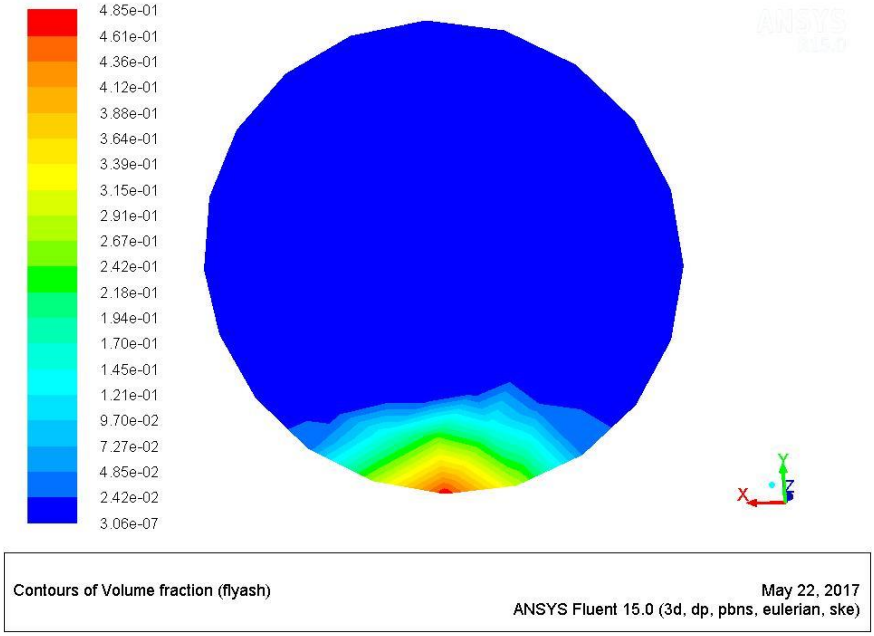

Solid volume fraction (100µm)

Figure 5.12: Contours of solid volume fraction for different particle diameter

5.15 Results of contours of volume fraction of flyash at different particle density

The results of contours of flyash at different particle density shows that as particle density increases the solid concentration at the bottom of the pipe also increases. Also the maximum volume fraction of flyash at particle density (1200kg/m3, 1700kg/m3 and 2200kg/m3) is same and is equal to 41.4% but solid volume fraction for particle density of 2700kg/m3 is 45.4% which is relatively more than solid volume fraction at lower densities. Higher solid volume distribution at the bottom of the pipe with increasing density suggests that heavier particle settles at the bottom due to high density as can be noticed in Fig. 5.13.

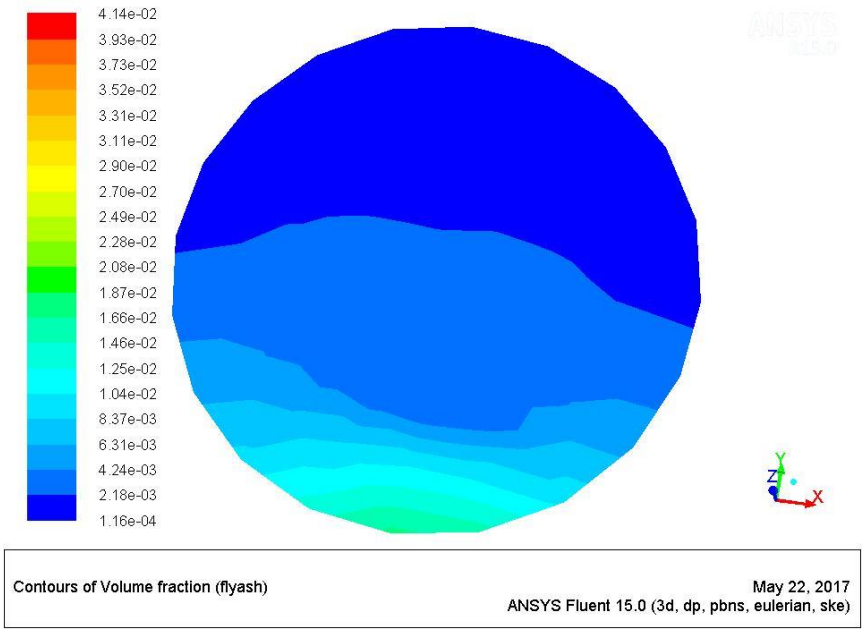

Particle density (1200kg/m^3)

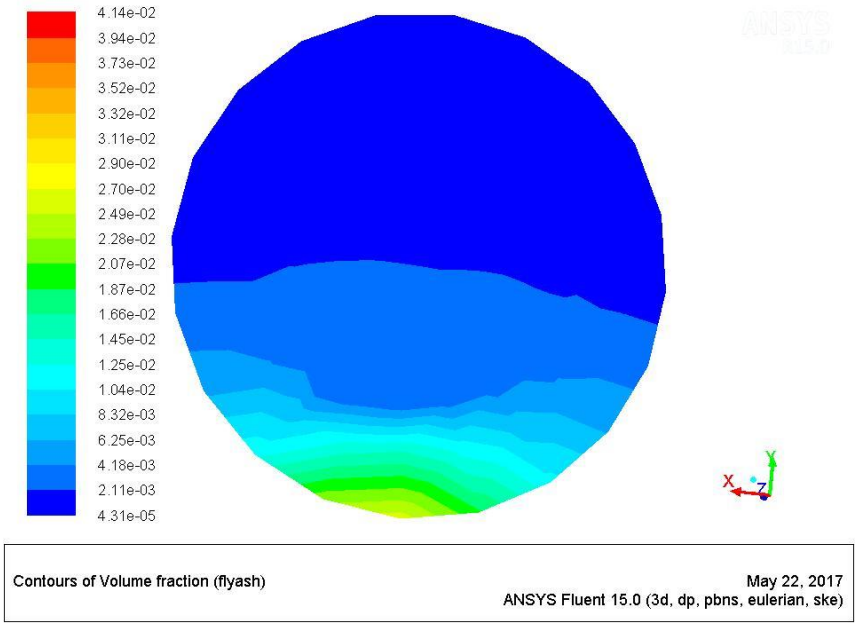

Particle density (1700kg/m^3)

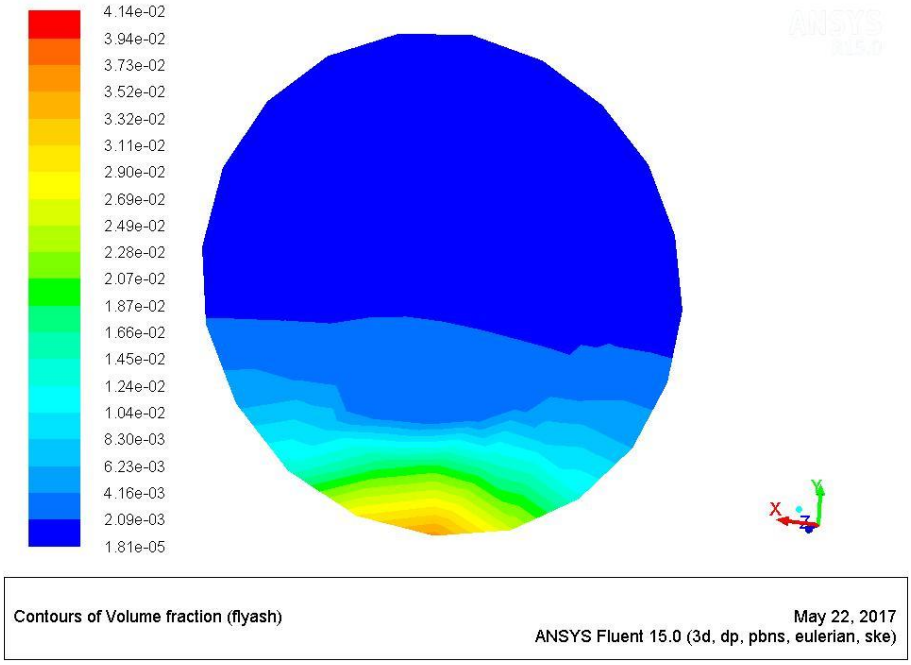

Particle density (2200 kg/m^3)

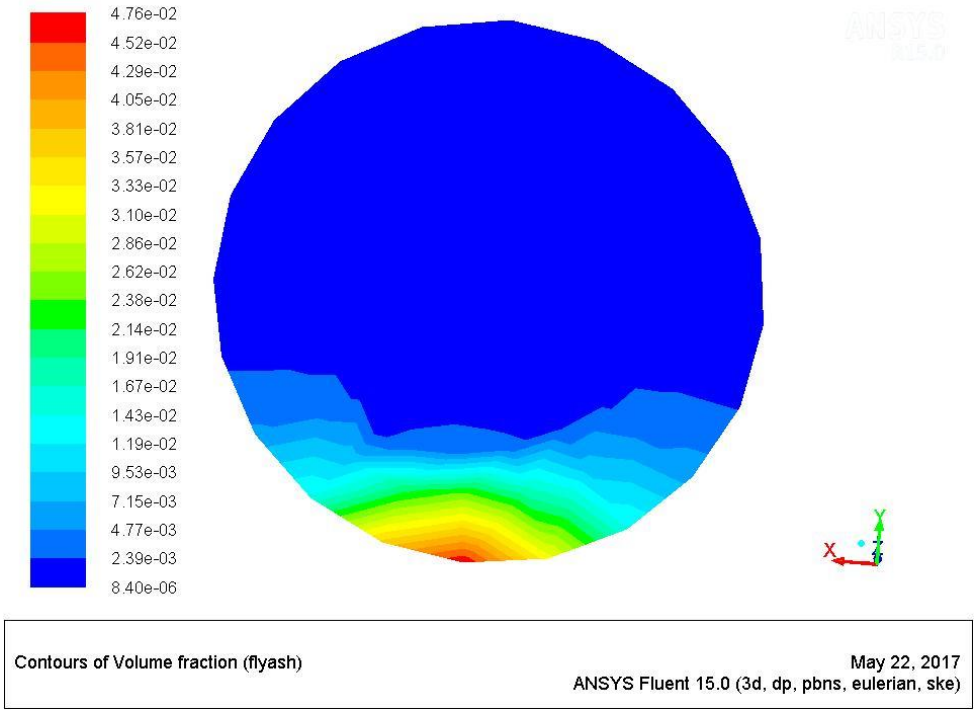

Particle density (2700kg/m^3)

Figure 5.13: Contours of solid volume fraction distribution at different particle density

Chapter 6

Conclusion and Future Scope

6.1 Conclusion

Based on the research work conducted in this study, it can be concluded that (CFD) simulation can be used for calculating the pressure drop for dense phase pneumatic conveying system. The results obtained for both the sets of straight pipes (69mm I.D. × 6m and 105mm I.D. ×6m) were quite close to the experimental results of pressure drop. The average errors of experimental and simulation pressure drop for both sets of simulation were 21.55% and 15.66 % respectively. The simulation PCC curves obtained after proper interpolation were showing almost the same trend as experimental PCC, though the length selected for the simulation was less than original length the results of pressure drop were appreciable. Thus it saved computation time for carrying out simulation on large length pipe. The computational study of effects of various parameters (such as particle diameter, particle density and particle volume fraction) keeping all other parameters constant resulted in following conclusions:

1) The pressure drop increases with particle diameter, it reaches peak value around mean particle diameter and then it decreases.
2) With the increase in particle density pressure drop increases.
3) The pressure drop increases linearly with particle volume fraction.

The study of the contours of flyash volume fraction at different particle density and particle volume fraction shows higher solid concentration at the bottom of the pipe at higher density and similarly solid concentration increases at the bottom of pipe for large diameter particle.

From the results of experimental PCC for grey cement and white cement it can be concluded that the single solid flow rate line was obtained since the variation of mass flow rate of solid was quite less (4.8t/h to 7.2t/h). Thus PCC for total pipeline pressure drop for grey and white cement is almost a horizontal line with small flow transition from dense phase.

6.2 Future Scope for Work

As discussed in Chapter 2, less research work is seen in open literature for predicting pressure drop in straight pipes and rare literature is provided on the PCC of the simulated pressure drop. This thesis was an attempt to check the capabilities of CFD software in predicting pressure drop in horizontal section of the pipe and the results obtained are close to the experimental values.

Still there is lot of scope for work in the field of pneumatic conveying utilising simulation capabilities for calculating pressure drop. There are some research areas in this field which require attention and have scope for future investigation:

1) Use of user defined codes in CFD for better prediction of pressure drop in both straight pipe and bend.
2) Simulation study of the effects of particle shape on pressure drop.
3) Bends are integral part of pneumatic conveying line which have inherited problems of roping, both experimental and simulation techniques should be used to address this issue in bends with the use of vortex breaker to suppress roping effects.
4) It is suggested that further studies should be made for the applicability of CFD simulation technique for predicting total pipeline pressure drop including both straight pipe and bends.

References

Barth, W., 1958. Strömungsvorgänge beim Transport von Festteilchen und Flüssigkeitsteilchen in Gasen. mit besonderer Berücksichtigung der Vorgänge bei pneumatischer Förderung. *Chemie Ingenieur Technik, 30*(3), pp.171-180.

Benyahia, S., Arastoopour, H., Knowlton, T. and Massah, H., 2000. Simulation of particles and gas flow behavior in the riser section of a circulating fluidized bed using the kinetic theory approach for the particulate phase. *Powder Technology, 112*(1), pp.24-33.

De Silva, S.R. and Datta, B.K., 1995. Transport of Particulate Materials-Dilute Phase Pneumatic Transport. *Lecture Notes on Powder Technology, Telemark University College, Porsgruun, Norway*.

Ding, J. and Gidaspow, D., 1990. A bubbling fluidization model using kinetic theory of granular flow. *AIChE journal, 36*(4), pp.523-538.

Giddings, D., Aroussi, A., Pickering, S.J. and Mozaffari, E., 2004. A 1/4 scale test facility for PF transport in power station pipelines. *Fuel, 83*(16), pp.2195-2204.

Jenkins, J.T. and Savage, S.B., 1983. A theory for the rapid flow of identical, smooth, nearly elastic, spherical particles. *Journal of fluid mechanics, 130*, pp.187-202.

Johanson, P.C. And Jackson, R., 1987. "Frictional-collision constitutive relation for granular materials, with application to plane shearing", *Journal of Fluid Mechanics*, 176, 67-93.

Jones, M.G. and Williams, K.C. 2003. Solids friction factors for fluidized dense phase conveying. *Particulate Science and Technology*. 21: 45-56.

Kartushinsky A.I., Michaelides E.E., Rudi Y.A., Tisler S.V., and Shcheglov I.N., 2011. Numerical simulation of three-dimensional gas-solid particle flow in a horizontal pipe. *AIChE Journal* 57, 2977–2988.

Klinzing, G.E., Rizk, F., Marcus, R. and Leung, L.S. 2009. *Pneumatic Conveying of Solids.*

Lain S. and Sommerfeld M., 2011. Numerical analysis of a pneumatic conveying system consisting of a horizontal pipe, 90º bend and vertical pipe. *Proceedings of the 12th International Conference on Multiphase Flow in Industrial Plants*. Paper No. 141, Ischia, Italy.

Lain S. and Sommerfeld M., 2012. Characterization of pneumatic conveying systems using the Euler/Lagrange approach. *Powder Technology* 235, 764–782.

Levy A. and Mason D.J., 2000. Two-layer model for non-suspension gas-solids flow in pipes. *Powder Technology* 112, 256–262.

Levy, A., Mooney, T., Marjanovic, P. and Mason, D.J., 1997. A comparison of analytical and numerical models with experimental data for gas-solid flow through a straight pipe at different inclinations. *Powder Technology*, *93*(3), pp.253-260.

Li, H. And Tomita, Y., 2000. A numerical simulation of swirling flow pneumatic conveying in a horizontal pipeline. *Particulate Science and Technology*, *18*(*4),* pp.275-291.

Liu, H. Pneumatic Casule Pipeline- Basic Concept, practical Considerations, and Current Research. in Mid-Continent Transportation Symposium. 2000. *Iowa State University, Ames, Iowa, USA*

Lun, C.K.K., Savage, S.B., Jeffrey, D.J. And Chepurniy, N., 1984. "Kinetic Theories for Granular Flow: Inelastic Particles in Couette Flow and Slightly Inelastic Particles in a General Flow Field", *Journal of fluid mechanics, 140*, 223-256.

Mallick, S.S. 2010. PhD Dissertation: Modelling of Fluidised Dense Phase Pneumatic Conveying of Powders University of Wollongong.

Manger, E., 1996. "Modelling and Simulation of Gas/Solids Flow in Curvilinear Coordinates", Ph.D. Thesis, *Process Technology, Telemark University College, Norway.*

Mason, D.J., Marjanovic, P. and Levy, A., 1998. A simulation system for pneumatic conveying systems. *Powder Technology*, *95*(1), pp.7-14.

Mathiesen, V. and Solberg, T., 2004. Laser-based flow measurements of dilute vertical pneumatic transport. *Chemical Engineering Communications*, *191*(3), pp. 414-433.

Mathiesen, V., 1997. *An Experimental and Computational Study of Multiphase Flow Behaviour in Circulating Fluidizing Beds* (Doctoral dissertation, Ph. D. Thesis, Process Technology, Telemark University College, Norway).

Pan, R. 1992. Improving scale-up procedures for the design of pneumatic conveying systems. Australia: *University of Wollongong (Doctoral dissertation)*

Pan, R., & Wypych, P. W. 1998. Dilute and dense phase pneumatic conveying of fly ash. In *Proceedings of the sixth international conference on bulk materials storage and transportation Wollongong, NSW, Australia*, (pp. 183–189).

Pan, R., 1992. Improving scale-up procedures for the design of pneumatic conveying systems.

Patankar S.V., 1980. Numerical heat transfer and fluid flow. *Hemisphere Publishing Corporation, Washington, DC*

Ratnayke, C. 2005. A Comprehensive Scaling up Technique for Pneumatic Transport Systems (Doctoral dissertation), *Norwegian University of Science and Technology (NTNU).*

Rizk, F., 1976. Pneumatic Conveying at Optimal Operation Conditions and a Solution of Barth's Equation λ_z= φ (λ_z, β). In *Proc. 3rd Int. Conf. Pneumat. Transport of Solids in Pipes, BHRA Fluid Eng.* (Vol. 4).

Rizk, F. 1982. Pneumatic Transport in dilute and dense phase. *Bulk Solids Handling*. (2): 235-241.

Scott, A.M., 1978. Pneumatic Transport of Granules. *Chemical Engineer-London*, (330), pp.189-190.

Sommerfeld M. and Kussin J., 2004. Wall roughness effects on pneumatic conveying of spherical particles in a narrow horizontal channel. *Powder Technology* 142, 180–192.

Sommerfeld, M., Lain, S. and Kussin, J., 2001. Analysis of transport effects of turbulent gas-particle flow in a horizontal channel. In *Proc. of 4th International Conference on Multiphase Flow*.

Stegmaier, W. 1978. Zur berechnung der horinentalen pneumatischen forderung feinkorniger feststoffe- for the calculation of horizontal pneumatic conveying of fine grained solids. *Fordern and Heben*. (28): 363-366.

Tsuji Y., Shen N.Y., and Morikawa Y., 1991. Lagrangian simulation of dilute gas-solid flows in a horizontal pipe. *Advanced Powder Technology 2*, 63–81.

Wang, Q., 2001. An Experimental and Computational Study of Gas/Particle Multiphase Flow in Process Equipment. *Telemark University College. Norway*.

Williams, K.C. and Jones, M.G., 2004, July. Numerical model velocity profile of fluidised dense phase pneumatic conveying. In *Proceedings of 8th International Conference on Bulk Materials Storage and Transportation* (pp. 354-358).

Wypych, P.W., 2006. Course note written on pneumatic conveying of bulk solids and dust control. *University of Wollongong*.

Wypych, P.W. 1989. PhD. Dissertation: Pneumatic Conveying of Bulk Solids. *University of Wollongong, Australia.*

Wypych, P.W. and Arnold, P.C. 1985. A standardised test procedure for pneumatic conveying design. *Bulk Solids Handling*. *5* (4): 755-763.

Yasuna, J.A., Moyer, H.R., Elliott, S. and Sinclair, J.L., 1995. Quantitative predictions of gas-particle flow in a vertical pipe with particle-particle interactions. *Powder Technology*, *84*(1), pp.23-34.

Ye, M., van der Hoef, M.A. and Kuipers, J.A.M., 2004. A numerical study of fluidization behavior of Geldart A particles using a discrete particle model. *Powder technology*, *139*(2), pp.129-139.

Zhu, K., Wong, C.K., Madhusudana Rao, S. and Wang, C.H., 2004. Pneumatic conveying of granular solids in horizontal and inclined pipes. *AIChE journal*, *50*(8), pp.1729-1745.

Web References

Sandy. 2017. A Brief History of Pneumatic Conveying. sandyhistorical.org. Retrieved 16 June 2017, from http://sandyhistorical.org/2016/02/09/a-brief-history-of-pneumatic-conveying

Buxton, Andrew 2004. Cash Carriers in Shops. Princes Risborough: Shire Publications. ISBN 978-0-7478-0615-8

D. Hamill, Sean 2012. "UPMC constructing underground pneumatic tubes to link hospitals to new lab". Pittsburgh Post-Gazette. Retrieved 10 January 2016

Steele, G. 2005. Dense Phase Pneumatic Conveying. www.dynamicair.com. Retrieved 16 June 2017, from http://www.dynamicair.com/pdf/worldcement.pdf

Reporters, T. 2017. 500mph Hyperloop train will travel from Dubai to Abu Dhabi in 12 minutes. The Telegraph. Retrieved 13 June 2017, from http://www.telegraph.co.uk/technology/2016/11/10/500mph-hyperloop-train-will-travel-from-dubai-to-abu-dhabi-in-12/

Patel, M. 2017. 7 Stages of a Typical CFD Simulation Available at: https://www.linkedin.com/pulse/20140703081437-225010003-7-stages-of-a-typical-cfd-simulation [Accessed 7 Mar. 2017]. Porsgruun, Norway. 2000 Publ. Springer. 3rd Ed.

Musk, Elon 2013. "Hyperloop Alpha" (PDF). SpaceX. Retrieved August 13, 2013.

Joseph Giotta 2003. "Transatlantic Tunnel". Extreme Engineering. Discovery Channel. Archived from the original on September 27, 2011

Appendix A

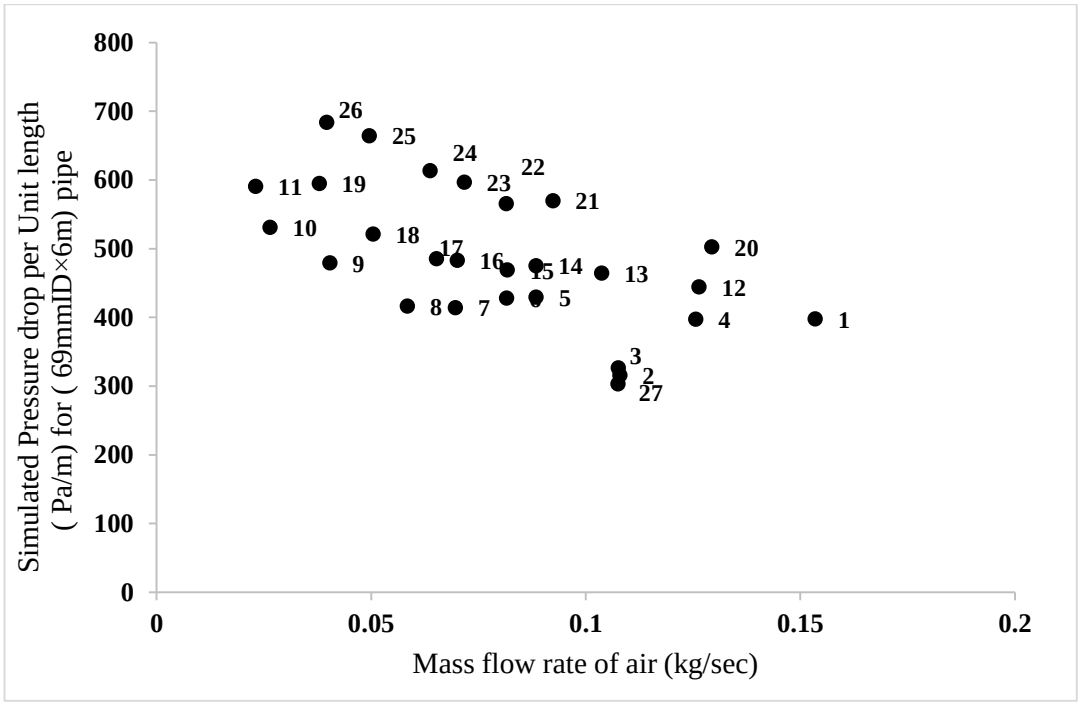

Figure A.1: Simulation Data points for PCC of 69 mm I.D. × 6m straight pipe

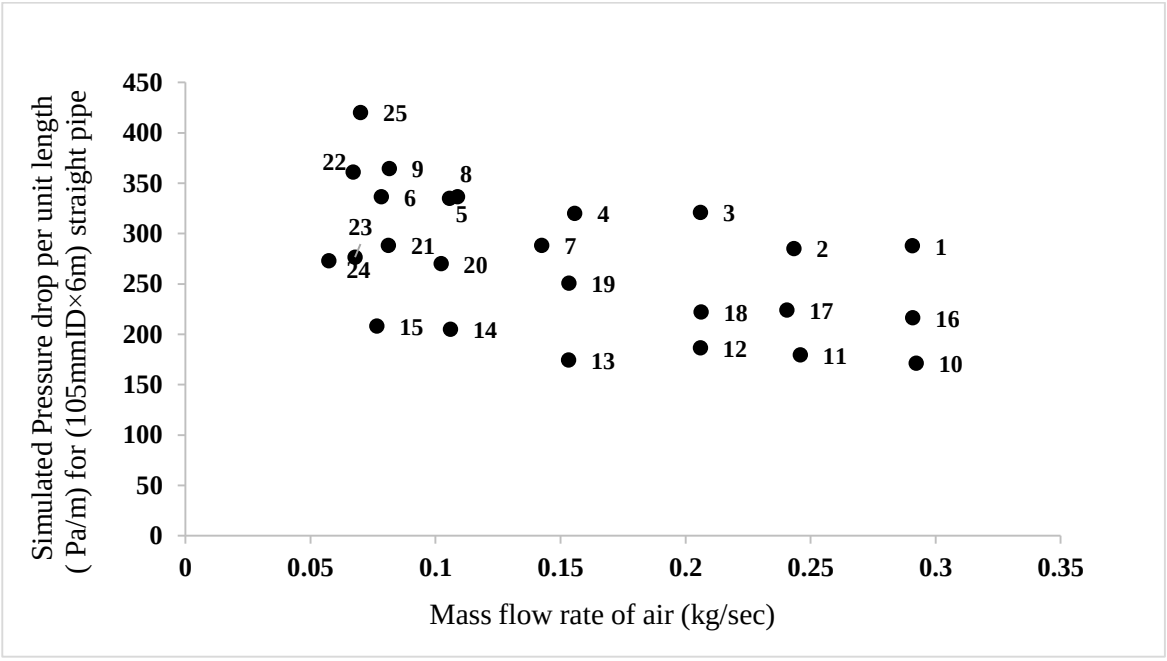

Figure A.2: Simulation data points for PCC of 105mm I.D. ×6m straight pipe

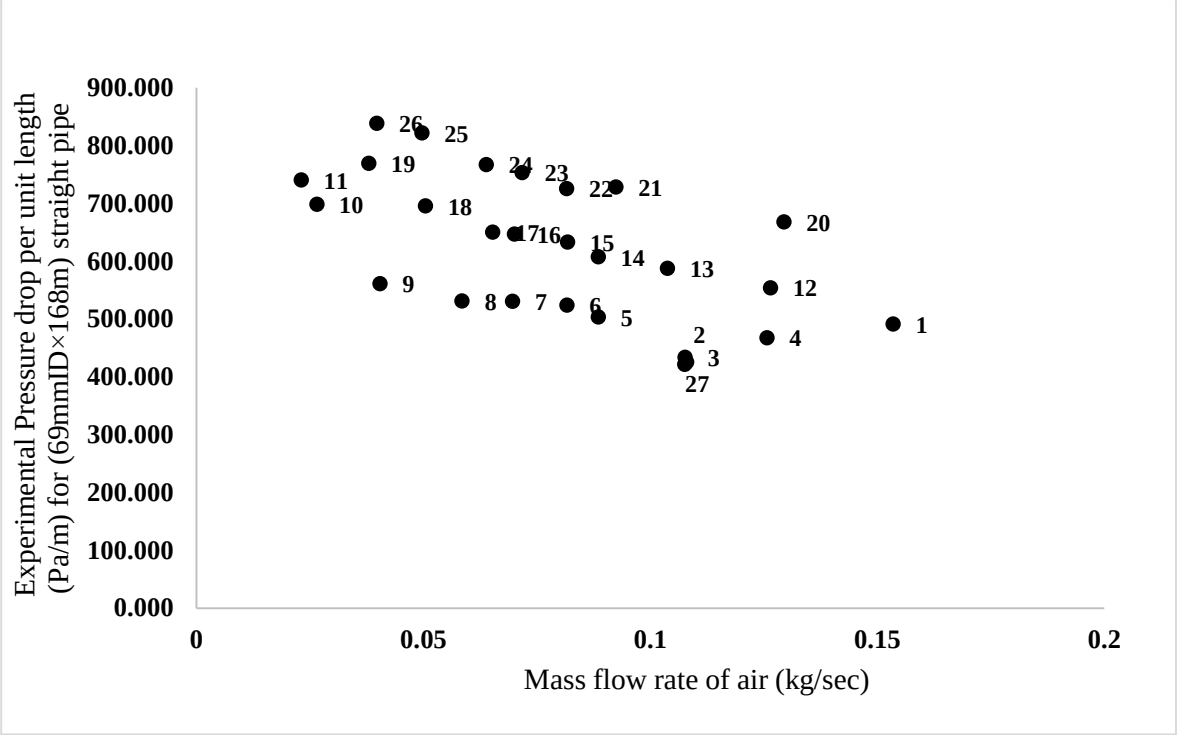

Figure A.3: Experimental data points for PCC of 69 mm I.D. × 168m straight pipe

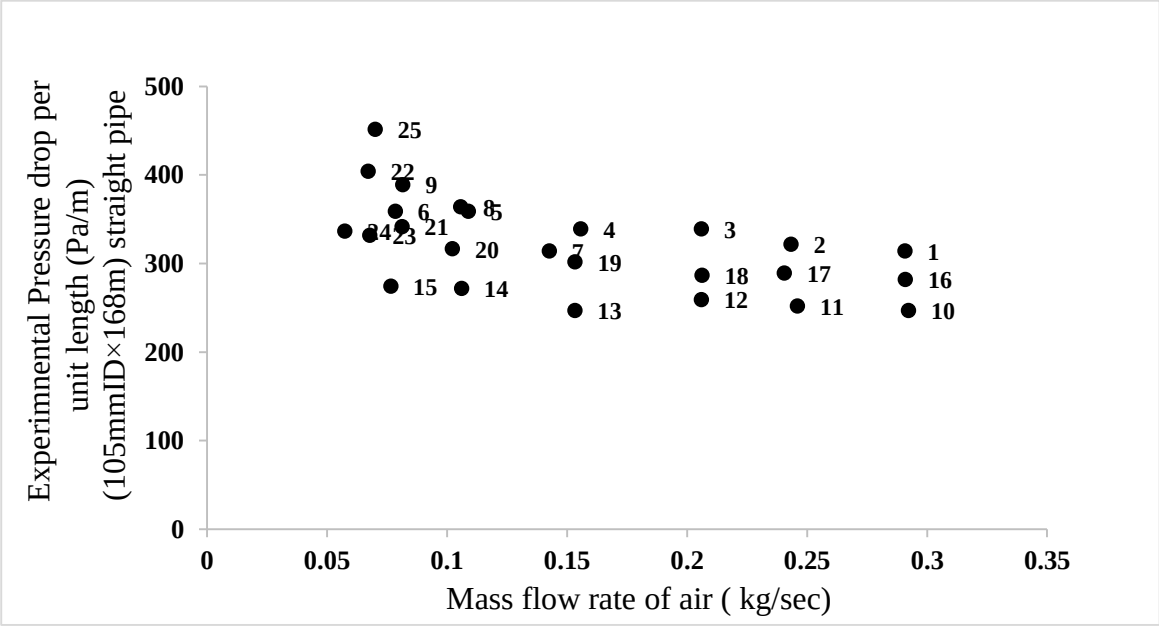

Figure A.4: Experimental data points for PCC of 105 mm I.D. × 168m straight pipe